A Study of 3-Substituted 7-Methoxy-2,3,4,5-tetrahydro-1*H*-benzo[*d*]azepin-1-ols Leading to Candidate PET Radioligands for Imaging Brain GluN2B: Design, Synthesis, and Structure–Activity Relationships

Lisheng Cai *, Leah Millard, Sean Costner, Alyssa Wang, Yonglan Liu, Victor W. Pike *

Posted Date: 17 April 2026

doi: 10.20944/preprints202604.0788.v2

Keywords: GluN2B; NMDA receptor; structure–activity relationship; radioligand; PET

 doi:10.20944/preprints202604.0788.v2

Article

A Study of 3-Substituted 7-Methoxy-2,3,4,5-tetrahydro-1*H*-benzo[*d*]azepin-1-ols Leading to Candidate PET Radioligands for Imaging Brain GluN2B: Design, Synthesis, and Structure–Activity Relationships

Lisheng Cai [1,*], Leah Millard [1], Sean Costner [1], Alyssa Wang [1], Yonglan Liu [2] and Victor W. Pike [1]

[1] PET Radiopharmaceutical Sciences Section, Molecular Imaging Branch, National Institute of Mental Health, National Institutes of Health, Bethesda, MD 20892, USA

[2] Bioinformatics and Computational Biosciences Branch, National Institute of Allergy and Infectious Diseases, National Institutes of Health, Bethesda, MD 20892, USA

* Correspondence: lishengcai@mail.nih.gov; Tel.: +(301)-451-3905; Fax: +(301)-480-5112

Abstract

N-Methyl-D-aspartate (NMDA) receptors are ligand- and voltage-gated ion channels essential for synaptic plasticity, learning, and memory. The GluN2B subunit, highly expressed in the forebrain and spinal cord, is implicated in multiple neurological and psychiatric disorders, making it an attractive target for positron emission tomography (PET) imaging. However, the development of selective GluN2B PET radioligands remains challenging. Here, we describe the design, synthesis, and evaluation of eighteen 3-alkylaryl derivatives of 7-methoxy-2,3,4,5-tetrahydro-1*H*-benzo[*d*]azepin-1-ol, including enantiomerically resolved compounds, as candidate PET radioligands. Structure–activity relationship studies show that binding affinity is largely insensitive to electronic and steric variation at the terminal aryl group but strongly dependent on alkyl linker length, with a four-carbon chain providing optimal affinity. Binding affinity does not correlate with calculated lipophilicity, suggesting hydrophobicity is not the primary determinant of receptor interaction. Absolute configuration was established using vibrational circular dichroism and infrared spectroscopy, and docking studies provided insight into enantiomer-specific binding modes. Two ligands, **L3** and **L6**, and their enantiomers exhibited high GluN2B affinity, favorable physicochemical properties, and suitability for carbon-11 labeling. PET imaging confirmed strong and specific brain binding of the radiolabeled compounds. These findings establish this scaffold as a promising platform for GluN2B PET ligand development.

Keywords: GluN2B; NMDA receptor; structure–activity relationship; radioligand; PET

Introduction

N-Methyl-D-aspartate (NMDA) receptors are ligand- and voltage- gated ion channels that mediate synaptic Ca^{2+} and Na^{+} influx and K^{+} efflux. They play central roles in synaptic plasticity, learning, and memory [1]. NMDA receptors are widely expressed throughout the central nervous system and are implicated in the pathophysiology of numerous neurological and psychiatric disorders, making them important therapeutic targets [2–4].

Functional NMDA receptors are hetero-tetrameric complexes assembled from GluN1, GluN2 (A–D), and GluN3 (A or B) subunits. The diversity of subunit composition generates receptor subtypes with distinct structural, physiological, and pharmacological properties. NMDA receptors possess multiple ligand-binding domains, including sites for L-glutamate, glycine/D-serine,

 doi:10.20944/preprints202604.0788.v2

polyamines, Mg^{2+}, Zn^{2+}, and channel blockers such as phencyclidine [1]. Clinically used NMDA-targeting drugs include memantine, which is approved for the treatment of Alzheimer's disease [5,6].

Among NMDA receptor subunits, GluN2B has attracted particular interest. GluN2B-enriched receptors are predominantly expressed in the forebrain and dorsal horn of the spinal cord and are implicated in schizophrenia, stroke, neurodegeneration, and neuropathic pain [7–9]. Selective targeting of GluN2B, rather than non-selective inhibition of NMDA receptors, offers the possibility of therapeutic efficacy while minimizing adverse effects, such as hallucinations, sedation, and cognitive impairment.

Positron emission tomography (PET) enables non-invasive quantification of specific molecular targets in the living brain using radiolabeled ligands. PET imaging therefore has substantial potential to elucidate disease mechanisms in neurological and psychiatric disorders [10–13] and to support drug development through target engagement studies [14,15]. Any radioligand for brain PET imaging must incorporate a short-lived positron emitter such as carbon-11 ($t_{1/2}$ = 20.4 min) or fluorine-18 ($t_{1/2}$ = 109.8 min) and satisfy stringent requirements regarding affinity, selectivity, lipophilicity, metabolic stability, and brain penetration [16–18]. PET radioligands for robustly quantifying brain GluN2B would serve as valuable tools for translational research and for drug development [19].

Despite decades of effort, the development of successful PET radioligands for NMDA receptors has proven challenging [19–21]. To date, only radioligands based on a 3-(4-phenylbutyl)-2,3,4,5-tetrahydro-1*H*-benzo[*d*]azepine-1,7-diol framework have demonstrated clearly displaceable GluN2B signals in vivo [22], with only [^{11}C](*R*)-Me-NB-1 (Chart 1) evaluated in humans [23].

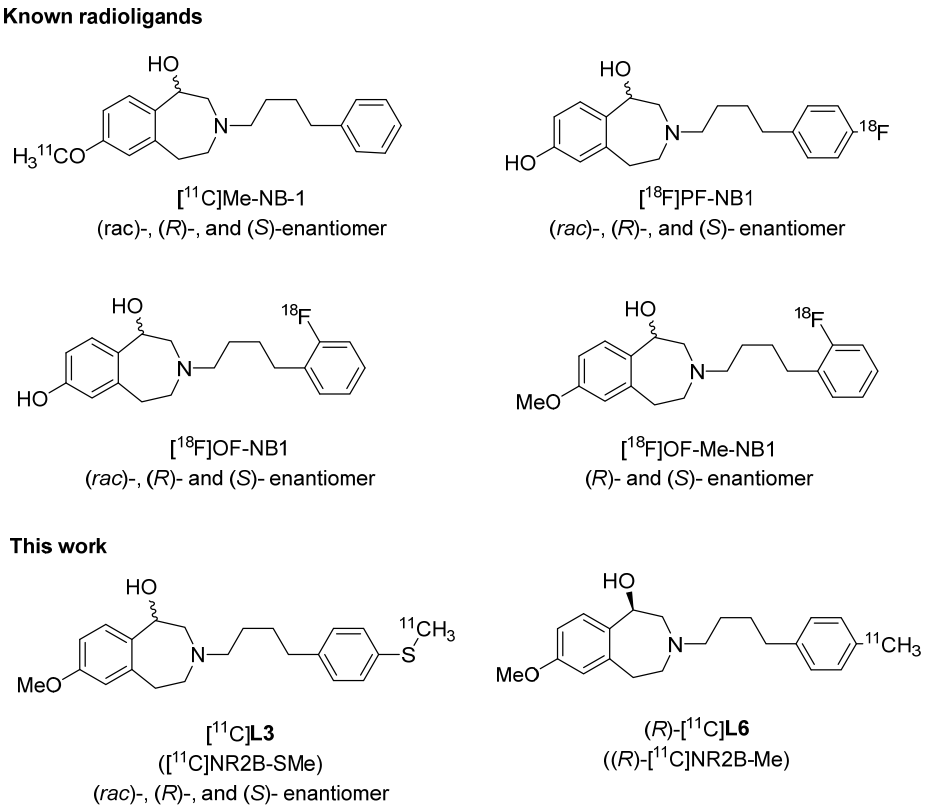

Chart 1. Radioligands evaluated for PET imaging of brain GluN2B in animals and humans.

Here we report our systematic investigation of structural variations at the 3-position of 7-methoxy-2,3,4,5-tetrahydro-1*H*-benzo[*d*]azepin-1-ol aimed at optimizing GluN2B ligands for PET imaging (Chart 2). Through synthesis and pharmacological evaluation of these derivatives, we sought to expand structure–activity knowledge and identify ligands with properties favorable for translation as GluN2B PET radioligands. This study produced the enantiomers of [^{11}C]NR2B-SMe

 doi:10.20944/preprints202604.0788.v2

([^{11}C]**L3**) [24] and [^{11}C]NR2B-Me ([^{11}C]**L6**) [25,26] (Chart 1), which exhibited nanomolar affinity for GluN2B, favorable lipophilicity, and suitability for carbon-11 labeling. In our separate studies, the [^{11}C]**L3** enantiomers demonstrated strong specific binding in rat brain [24], and [^{11}C](*R*)-**L6** showed high binding potential in monkey [26].

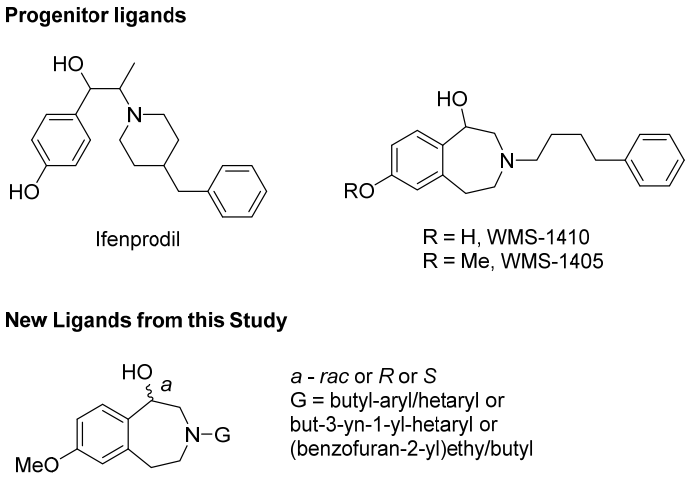

Chart 2. Progenitor GluN2B ligands and new ligands described in this study.

Results and Discussion

Ligand design. X-ray crystallography [27] has shown that the prototypical GluN2B ligand, ifenprodil (Chart 2), binds at the interface of GluN1 and GluN2B subunits in the NMDA receptor [28] by forming interactions critical for affinity and subtype selectivity. Key interactions include hydrogen bonding between the phenolic hydroxyl group and Glu236, and between the protonated amine and Gln210 of GluN2B. Additional aromatic and hydrophobic interactions involving residues from both GluN1 and GluN2B further stabilize binding (see Supporting Information for docking of (1*S*,2*R*)-ifenprodil to GluN2B/GluN1).

A chemical scaffold underlying many recent GluN2B ligands derives from WMS-1410, a conformationally constrained analogue of ifenprodil (Chart 2). WMS-1410 preserves key pharmacophoric elements while enhancing GluN2B selectivity [29]. Docking studies have indicated that WMS-1410 adopts a similar GluN2B binding pose to ifenprodil [30]. Importantly, the 2,3,4,5-tetrahydro-1*H*-benzo[*d*]azepine-1,7-diol scaffold of WMS-1410 confers high affinity and selectivity for GluN2B over other NMDA receptor subtypes and over a broad panel of off-target proteins [31,32].

The phenolic hydroxy group in WMS-1410 undergoes glucuronidation in vivo, limiting bioavailability [33]. Replacement of the 7-hydroxy group with a methoxy group, as in WMS-1405 (Chart 2), blocks glucuronidation and introduces a convenient site for ^{11}C-methylation. (*R*)-[^{11}C]Me-NB-1, a radiolabeled derivative of WMS-1405, demonstrated high GluN2B affinity and specific binding in vivo [23,34], Thus, the 7-methoxy substitution of WMS-1405 represents a viable platform for GluN2B PET radioligand development.

Both ifenprodil and WMS-1410 exhibit pronounced stereoselectivity: (1*R*,2*R*)-ifenprodil displays approximately 2.5-fold higher affinity (K_i = 5.8 nM) than its (1*S*,2*S*) antipode [36], whereas the *R*-enantiomer of WMS-1410 (K_i = 30 nM) is substantially more potent than the *S*-enantiomer (K_i = 740 nM) [33]. These findings underscore the importance of stereochemical orientation for productive binding within the GluN2B allosteric site.

N-Substituted 7-hydroxy and 7-methoxy derivatives of 2,3,4,5-tetrahydro-1*H*-benzo[*d*]azepin-1-ol and their enantiomers are among the most potent and selective GluN2B ligands. These scaffolds have served as the basis for several candidate PET radioligands, not only [^{11}C](*R*)-Me-NB-1 [23,34], but also [^{18}F](*S*)-oF-NB1 [26], and [^{18}F]PF-NB1 [35,36] (Chart 1). Here we built on this scaffold in a search for improved PET radioligands.

 doi:10.20944/preprints202604.0788.v2

This study is the first systematic evaluation of alkyl tether length and terminal aryl substitution at the 3-position in this scaffold. We focused on systematic modification of the alkyl-tethered terminal aryl group. Specifically, we examined: (i) the effect of para-substitution on the terminal phenyl ring, (ii) variation in alkyl linker length to probe spatial tolerance within the binding pocket, and (iii) introduction of unsaturation within the linker to modulate conformational flexibility and electronic properties (Chart 2). Through these targeted structural variations, we sought to refine structure–activity relationships and identify ligands optimized for high-affinity binding, favorable physicochemical properties, and suitability for PET radiolabeling.

Ligand syntheses. The overall strategy for ligand synthesis was to couple a requisite alkyl tosylate with 7-methoxy-2,3,4,5-tetrahydro-1*H*-benzo[*d*]azepin-1-ol (Scheme 1). Tosylates were prepared from the corresponding alcohols that were either purchased directly or obtained by various methods from commercially available starting materials, as described in Supporting Information.

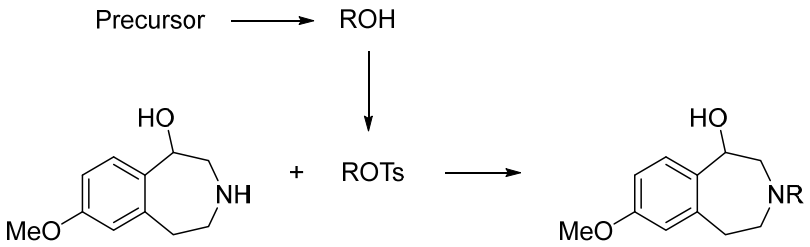

Scheme 1. Strategy for ligand synthesis.

Treatment of the synthesized alcohols with tosyl chloride in the presence of base gave the tosylates, **T1–T18,** in yields ranging from 13 to 77% (Scheme 2). Some reactions did not go to completion even with excess reagent. A long reaction time risked reduced yield from substitution of the tosylate group from product by the chloride anion generated from the tosyl chloride. Normally, overnight reactions gave the best compromise between yield and purity.

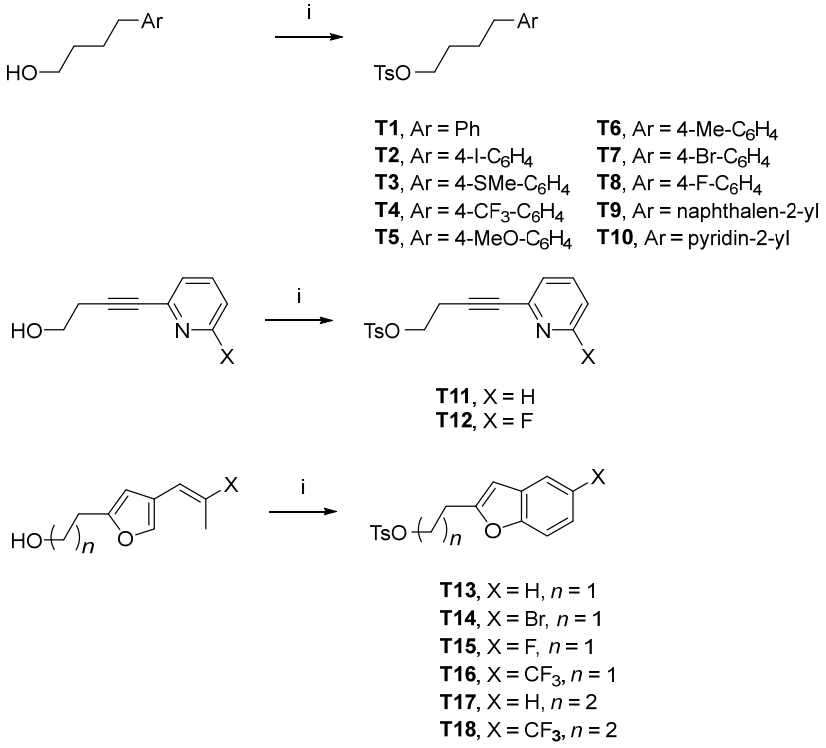

Scheme 2. Syntheses of tosylates **T1–T18**.

 doi:10.20944/preprints202604.0788.v2

Reagents, conditions, and yields: (i) TsCl, Et_3N, DCM, RT, overnight–24 h (**T1**, 77%; **T2**, 61%; **T3**, 47%; **T4**, 74%; **T5**, 21%; **T6**, 24%; **T7**, 58% after 5 d stirring; **T8**, 52%; **T9**, 22%; **T10**, 21%; **T11**, 22%; **T12**, 13%; **T13,** 45%; **T14**, 54%; **T15**, 72%; **T16**, 39%; **T17**, 76%; **T18**, 56%.

For the syntheses of the prospective GluN2B ligands, treatment of the prepared tosylates with 7-methoxy-2,3,4,5-tetrahydro-1*H*-benzo[*d*]azepin-1-ol was generally successful (Scheme 3), except in two cases, namely **L10** and **L12**, which likely resulted in competing cyclization reactions.

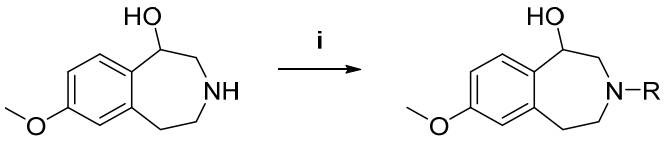

ii

L1 (WMS 1405): R = 4-(phenyl)butyl
L2: R = 4-(4-iodophenyl)butyl
L3: R = 4-(4-methylthiophenyl)butyl
L4: R = 4-(4-trifluoromethylphenyl)butyl
L5: R = 4-(4-methoxyphenyl)butyl
L6: R = 4-(4-methylphenyl)butyl
L7: R = 4-(4-bromophenyl)butyl
L8: R = 4-(4-fluorophenyl)butyl
L9: R = 4-(naphthalen-2-yl)butyl
L10: R = 4-(pyridin-2-yl)butyl (unsuccessful)
L11: R = 4-(pyridin-2-yl)but-3-yn-1-yl
L12: R = 4-(6-fluoropyridin-yl)but-3-yn-1-yl
L13: R = 2-(benzofuran-2-yl)ethyl
L14: R = 2-(5-bromobenzofuran-2-yl)ethyl
L15: R = 2-(5-fluorobenzofuran-2-yl)ethyl
L16: R = 2-(5-trifluromethylbenzofuran-2-yl)ethyl
L17: R = 4-(benzofuran-2-yl)butyl
L18: R = 4-(5-(trifluromethyl)benzofuran-2-yl)butyl
L19: R = methyl 3-((4-butylphenyl)thio)propanoate

Scheme 3. Syntheses of racemic ligands **L1–L9** and **L11–L19**.

Reagents, conditions and yields: (i) ROTs (**T1**), K_2CO_3, MeCN, 6 d at reflux. (**L1**, 72%). (ii) ROTs (**T2**), K_2CO_3, MeCN, 5 d at 75 °C. (**L2**, 73%). (iii) ROTs (**T3** or **T4**), K_2CO_3, MeCN, 2 d at 75 °C. (**L3**, 75%; **L4**, 71%). (iii) ROTs (**T5**, **T6**, or **T8)**, K_2CO_3, MeCN, 2 d at 90 °C. (**L5**, 87%; **L6**, 37%; **L8**, 79%). (iv) ROTs (**T7**, **T9**, or **T11**), K_2CO_3, MeCN, 5 d at 90 °C. (**L7**, 62%; **L9**, 74%; **L11**, 77%). (iv) ROTs (**T12**, **T14**, **T15**, **T16**, **T17**, or **T18**) MW (135 °C, 10 min, 60 W, 250 psi). (**L12**, 12%; **L14**, 51%; **L15**, 59%; **L16**, 64%; **L17**, 71%; **L18**, 68%). (v) ROTs (**T13**), Na_2HPO_4, MeCN, 22 d at 90 °C. (**L13**, 71%). (ii) **L2**, methyl 3-mercaptopropanoate, *N*,*N*,1,1,1-pentamethylstaannanamine, $Pd(PPh_3)_4$, DMSO, MW (110 ℃, 50 W, 250 psi) **(L19**, 86%).

When **T10** (R = 4-(pyridin-2-yl)butyl) was used in the synthesis, only an unexpected byproduct was observed (Scheme 4). LC-MS indicated that this was a cyclic product from an intramolecular attack on the tosylate group by the nucleophilic pyridinyl nitrogen. Changing the concentration of **T10**, including the use of pure **T10** as solvent, did not generate any of the desired ligand (**L10**). No further attempt was made to synthesize **L10**.

Reagents, conditions and yields: (i) Na_2HPO_4, DMSO, MW (80 °C, 10 min, 30 W, 250 psi, or 120 °C, 10 min, 50 W, 250 psi, or 150 °C, 10 min, 60 W, 250 psi). (No **L10**; putative cyclized product only); (ii) Na_2HPO_4, MeCN, 90 °C for 22 d. (No **L10**; putative cyclized product only).

 doi:10.20944/preprints202604.0788.v2

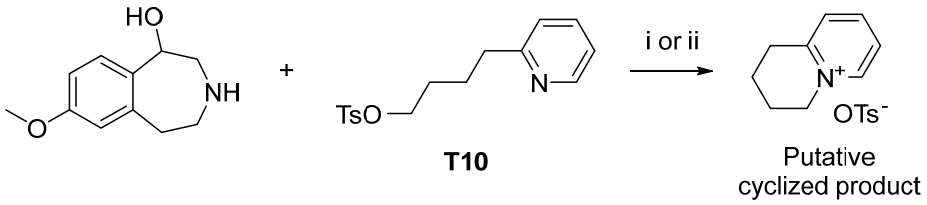

Scheme 4. Attempted synthesis of **L10**.

When 7-methoxy-2,3,4,5-tetrahydro-1*H*-benzo[*d*]azepin-1-ol was treated with **T12** in the presence of disodium hydrogen phosphate as base, **L12** was produced in low yield. An appreciable by-product was also obtained. This was probably a cyclic product from intramolecular substitution of the 6-fluoro group by the remote hydroxy group (probably as its phenoxide) in **L12**. The use of other bases, such as sodium carbonate or bicarbonate, did not improve the yield of **L12**. These outcomes further underscore the possible susceptibility of pyridinyl-containing tosylates to intramolecular cyclization, as likely seen in the attempted synthesis of **L10**

Precursors for ^{11}C-labeling. The methyl arylthiopropanoate esters **L19** and its enantiomers were synthesized from **L2** and its enantiomers, respectively and purified by preparative chiral HPLC (see Experimental and Supporting Information) (Scheme 5).

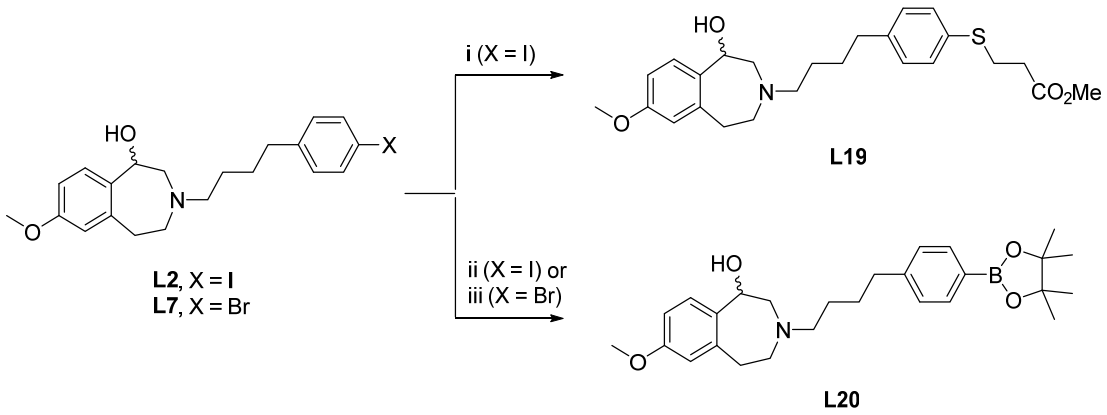

Scheme 5. Syntheses of precursors **L19** and **L20**.

Reagents, conditions, and yields: (i) Methyl-3-mercaptopropanoate, *N*,*N*,1,1,1-pentamethylstannanamine, $Pd(Ph_3)_4$, DMSO, MW (110 ℃, 10 min, 50 W, 250 psi). (86% from **L2**). (ii) 4,4,4',4',5,5,5',5'-Octamethyl-2,2'-bi(1,3,2-dioxaborolane), DPPF-$PdCl_2$•CH_2Cl_2, DMSO, MW (80 °C, 60 min, 60 W, 250 psi). (37% from **L2**). (iii) 4,4,4',4',5,5,5',5'-Octamethyl-2,2'-bi(1,3,2-dioxaborolane), DPPF-$PdCl_2$●CH_2Cl_2, DMSO, MW (110 °C, 30 min, 50 W, 250 psi). (54% from **L7**).

L20 was synthesized by substitution of either the iodo or bromo substituent in **L2** or **L7**, respectively, with Bpin using DPPF-$PdCl_2$●CH_2Cl_2 as catalyst under microwave heating conditions (Scheme 5). The enantiomers of **L20** were obtained by chiral resolution (see Experimental and Supporting Information).

Absolute configuration correlation. We used vibrational circular dichroism/infrared (VCD/IR) plus quantum calculations to determine the absolute configuration of the enantiomers of ligand **L3** (see Supporting Information) [24]. Four homochiral ligands (enantiomers of **L2**, **L6**, **L19**, and **L20**) were related to (*S*)-**L3** through stereo-retentive chemical reactions, thereby allowing unequivocal assignment of their absolute configurations (Scheme 6). In each case, we observed that the early eluting enantiomers of these ligands on chiral HPLC analysis with the (*S*,*S*)-Whelk column had the same absolute configuration, which we determined to be *S*. We also observed that each enantiomer

 doi:10.20944/preprints202604.0788.v2

of **L3** has opposite specific optical rotation sign in ethanol and chloroform (see Experimental), which had to be considered in the VCD/IR analysis.

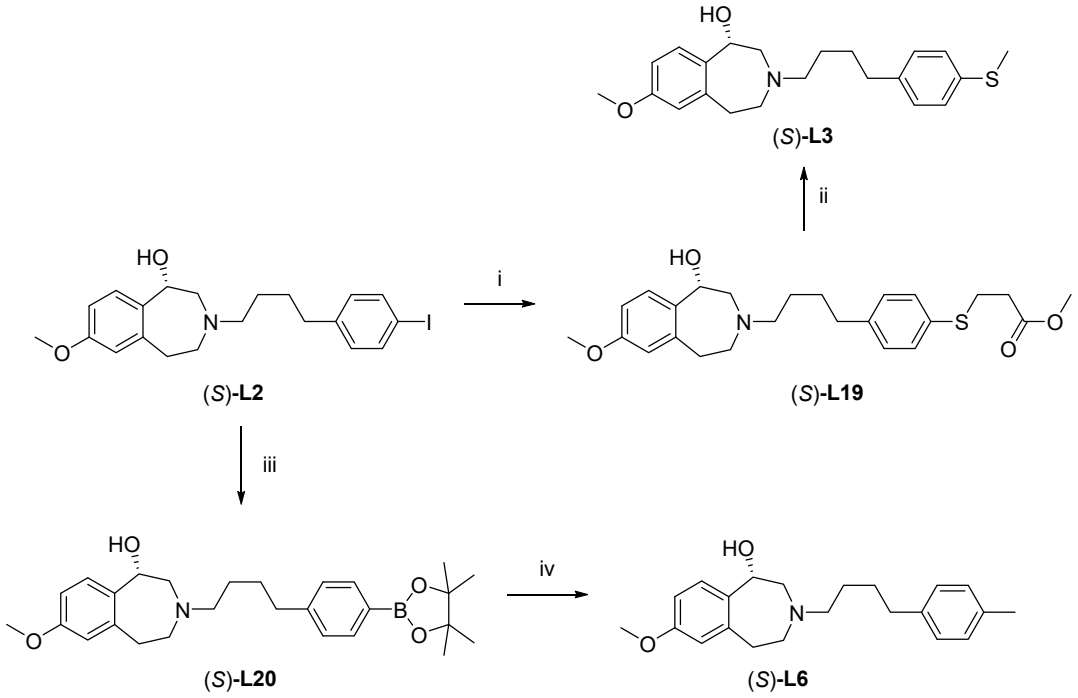

Scheme 6. Determination of the absolute configurations of **L3**, **L6**, **L19**, and **L20** enantiomers by relation to the absolute configuration of (*S*)-**L3**, determined by VCD/IR and stereo-retentive reactions.

Reagents, conditions, and yields: (i) Methyl 3-((trimethylstannyl)thio)propanoate, Pd(DPPF)Cl_2, Et_3N, MeCN, MW (90 °C, 20 min, 120 W, 250 psi). 84% (ii) MeI, TBAOH, DCM, rt, 20 min. 75%. (iii) Bis(pinacolato)diboron, KOAc, Pd(DPPF)Cl_2, MeCN, MW (80 °C. 20 min, 150 W, 250 psi). 31%. (iv) MeI, CsF, $Pd(PPh_3)_4$, MeOH/MeCN, MW (90 °C. 20 min, 80 W, 250 psi). 84%.

The chemical transformations shown in Scheme 6 did not cause any appreciable racemization of the products formed from homochiral starting materials.

Ligand structure versus affinity for GluN2B. 19 racemic ligands and a few enantiomers were variously evaluated for binding to rat brain GluN2B through in vitro binding assays with [^{3}H]ifenprodil as reference radioligand, including the manual and automatic assays at the Psychoactive Drug Screening Program (PDSP) and an in-house binding assay with rat brain homogenate (Tables 1). Nonetheless, the results are useful for ranking and comparing binding affinities for the whole set of ligands. Thus, the manual PDSP assay gave three to tenfold lower K_i values than the automated assay, but a similar ranking of ligand affinities. Thus, the in-house assay gave lower K_i values than either PDSP assay.

We systematically varied substituents on the terminal aryl group and the length and composition of the alkyl linker to define structure–activity relationships within this series. Among ligands bearing a para-substituted phenylbutyl group (**L2–L8**), binding affinities varied only modestly (20–44 nM) across a range of substituents (SMe, OMe, H, Me, Br, F), indicating that the GluN2B binding pocket is largely insensitive to electronic and steric variation at the aryl terminus. Even bulky substituents, such as naphthalenyl (**L11**), were well tolerated. In contrast, introduction of a terminal hydrogen bond acceptor (e.g., pyridinyl groups in **L11** and **L12**) markedly reduced affinity, consistent with a predominantly hydrophobic interaction in this region of the binding pocket.

 doi:10.20944/preprints202604.0788.v2

Table 1. K_i values for the binding of ligands **L1–L9** and **L11–L19** to rat brain GluN2B, clog*D* values, and CNS PET MPO scores.

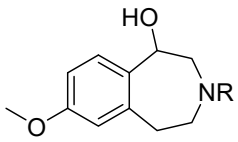

Ligand	R	K_i from automated PDSP assay[a] (nM)	K_i from manual PDSP assay[a] (nM)	K_i from in-house assay[b] (nM)	clog*D*[c]	CNS PET MPO[d]
L1 (WMS 1405)	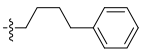	44 ± 7	9.8 ± 2	263 ± 50	3.13	2.5
L2	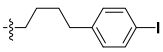	21 ± 4	2.2	1272 ± 250	4.12	1.7
L3 (NR2B-SMe)	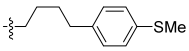	20 ± 5	2.0[e]		3.39[e]	1.8
(*S*)-**L3**	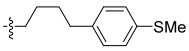			13 ± 3	3.39	1.8
L4	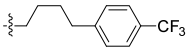			309 ± 60	3.83	1.7
L5	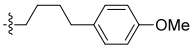	44 ± 9	9 ± 2		2.90	2.9
L6 (NR2B-Me)	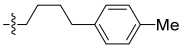	31 ± 5	4.9 ± 1[f]		3.34	2.0
(*S*)-**L6**	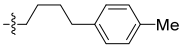			78 ± 15	3.34	2.0
(*R*)-**L6**	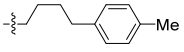			138 ± 30	3.34	2.0
L7	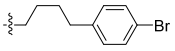	27 ± 5	2.5 ± 0.5		3.90	1.7
L8	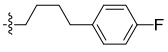	28 ± 6	3.7 ± 0.4		3.17	2.0
L9	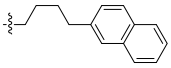	23 ± 6	7 ± 2		4.53	1.7
L11	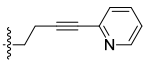	493 ± 100	97 ± 20		3.20	3.7
L12	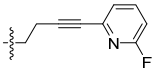	584 ± 100	129 ± 20		3.86	3.0
L13	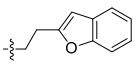	120 ± 24		1674 ± 300[g]	2.59	3.7
L14	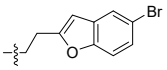	66 ± 14			4.41	2.5

 doi:10.20944/preprints202604.0788.v2

L15	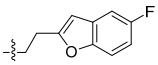	54 ± 14	2213 ± 400g[g]	3.68	2.5
L16	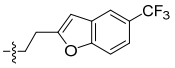	49 ± 12	288 ± 50[g]	4.39	2.5
L17	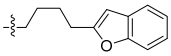	44 ±12		3.14	2.7
L18	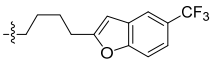	19 ± 4		3.67	2.5
L19	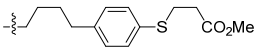	42 ± 9		3.23	2.9

[a] Assays were performed by the Psychoactive Drug Screening Program with cells overexpressing GluN2B (see Experimental). [b] From in-house assay (see Experimental. Ro 25-6981 gave K_i values between 10 and 26 nM in the in-house assay). [c] Calculated from Pallas software. [d] Calculated according to the literature [17]. [e] First reported in Cai *et al*. [24]. [f] Measured to be 3.41 [25]. [g] Ro 25-6981 had a K_i of 13 ± 4 nM in the same assay session. All assay results are mean ± SD for $n \geq 3$.

In contrast to the limited influence of aryl substitution, linker length had a pronounced effect on binding affinity. Comparisons across series (e.g., **L13** vs **L17** and **L16** vs **L18**) indicate that a flexible four-carbon tether provides optimal positioning of the terminal aryl group within the binding site. Shorter or more constrained linkers resulted in reduced affinity, highlighting the importance of spatial alignment over electronic effects in governing ligand–receptor interactions.

Notably, counter to typical CNS ligand expectations, no meaningful correlation was found between binding affinity and calculated lipophilicity (clog*D*) (see Supporting Information, Figure S120). This indicates that global hydrophobicity is not a dominant determinant of binding. This finding further supports the view that specific geometric and local interactions, rather than bulk physicochemical properties, govern productive engagement with the GluN2B binding pocket.

Together, these results identify linker length as the primary determinant of affinity in this series, with the binding pocket exhibiting substantial tolerance to variation in terminal aryl substitution.

Ligand binding poses and interactions with the target GluN2B complex. Molecular docking was performed to predict the binding poses and the interactions of **L3** and **L6** with the GluN1a/GluN2B complex. The protonated amine in both the *R*- and *S*-configurations of **L3** (Figure 1a) and **L6** (Figure 1b) forms a hydrogen bond with Gln110 of GluN2B, consistent with the interaction observed in ifenprodil binding (Supporting Information Figure S118). The hydroxyl group adopts distinct orientations depending on stereochemistry. In the *S*-configuration, the hydroxyl group is oriented toward GluN1a and forms hydrogen bonds with the backbone of Ser132 in GluN1a and with Gln110 of GluN2B, in agreement with the X-ray structure of the ifenprodil-bound complex [27]. In contrast, in the *R*-configuration, the hydroxyl group flips in the opposite direction and forms a hydrogen bond with Glu106 of GluN2B. Another conserved interaction is the π–π stacking between the benzene ring of the methoxyphenyl group and Phe176 of GluN2B within the binding pocket. In ifenprodil, the phenolic hydroxyl group forms a hydrogen bond with Glu236 of GluN2B. However, in **L3** and **L6**, this group is replaced by a methoxy substituent, resulting in the loss of this interaction. The variable regions of **L3** and **L6** participate in conserved hydrophobic interactions with Ala75, Pro106, and Tyr109 of GluN1a, as well as Ile82, Ile111, Phe114, and Pro78 of GluN2B.

 doi:10.20944/preprints202604.0788.v2

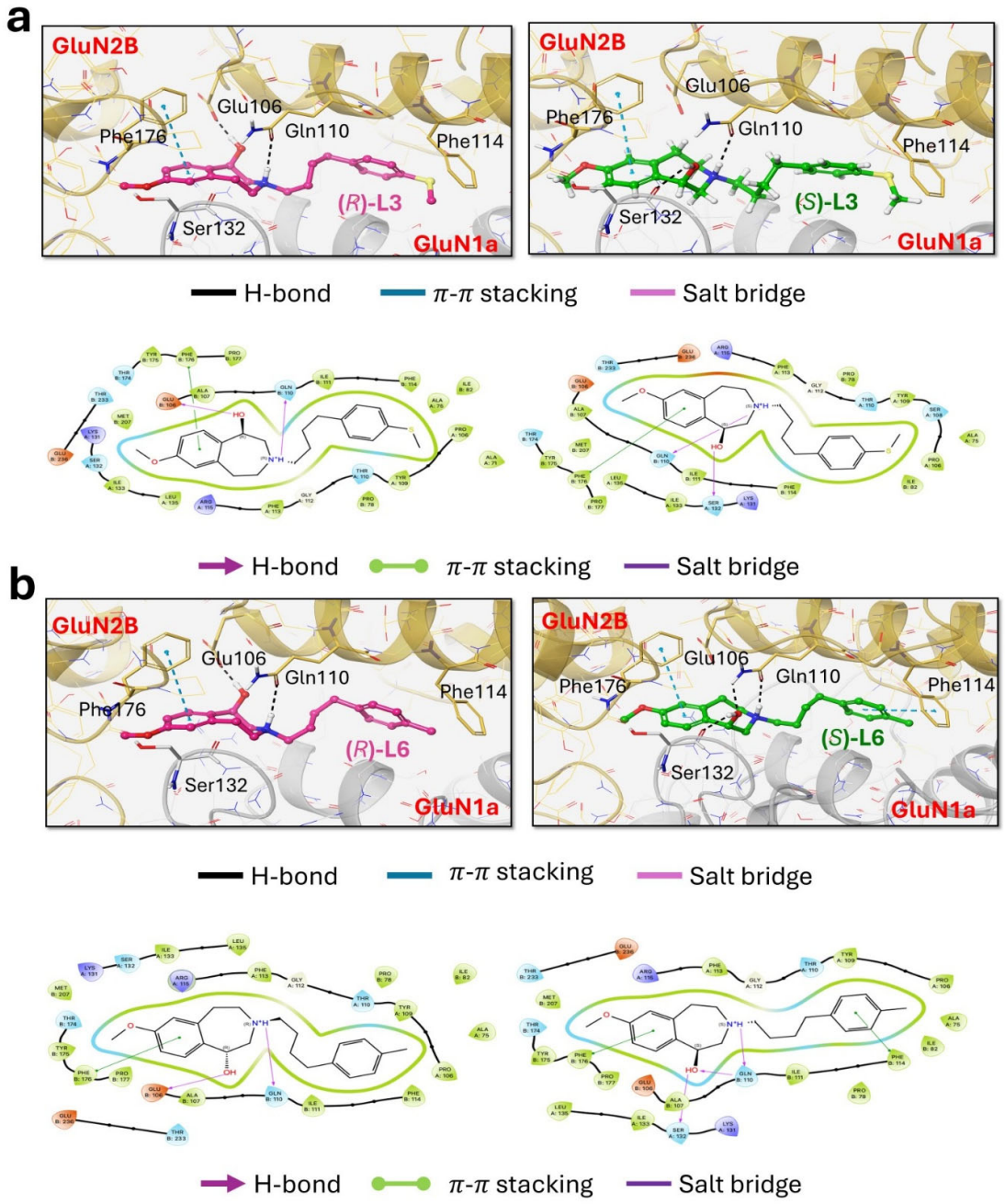

Figure 1. Binding poses and interactions of (**a**) (*R*)- and (*S*)-**L3** and (**b**) (*R*)- and (*S*)-**L6** with the GluN1a/GluN2B complex. In the 3D interaction representations, GluN1a and GluN2B are shown in light gray and yellow, respectively, and residues involved in key interactions are highlighted as sticks. In the 2D interaction diagrams, positively charged, negatively charged, hydrophobic, and hydrophilic residues are colored dark orange, blue, green, and cyan, respectively.

L19 contains a long terminal *p*-S-$CH_2CH_2CO_2Me$ group that might extend toward Phe114 of GluN2B, potentially leading to steric clashes. However, **L19** still exhibits high binding affinity (Table 1). This suggests that **L19** may adopt a distinct binding mode or interaction pattern within the pocket. To account for receptor flexibility during ligand binding, Induced Fit Docking (IFD) was applied. As expected, the resulting binding poses of **L19** were diverse, with the long terminal *p*-S-$CH_2CH_2CO_2Me$ group displaying significant conformational flexibility (Supplementary Figures 121 and 122). In the binding, in addition to hydrogen bond interactions involving the protonated amine and hydroxyl

 doi:10.20944/preprints202604.0788.v2

group of **L19** with Gln110 of GluN2B (and) Ser132 of GluN1a (observed for (*S*)-**L19**), the central benzene ring adopts a rotated orientation that enables π–π stacking with Tyr109 of GluN1a (Supplementary Figures 121b and 122b). Furthermore, the protonated amine is likely to form a salt bridge with Glu106 of GluN2B. The terminal carbonyl oxygen might be able to position in a region favorable for hydrogen bonding with Gln110 (Supplementary Figures 121c and 122c).

Overall, these results indicate that **L3** and **L6** largely preserve the key interaction network observed for ifenprodil, whereas **L19** adopts a more flexible binding mode that accommodates its extended substituent without compromising binding affinity.

PET radioligand selection and synthesis. From a total of eighteen new ligands prepared in this study, we selected two ligands and their enantiomers for labeling with carbon-11 and evaluation as GluN2B PET radioligands in animals, namely **L3** (NR2B-SMe) [24] and **L6** (NR2B-Me) [25]. These two ligands were selected based on a combination of their high affinities for GluN2B, acceptable lipophilicities (moderate clog*D* values), acceptable CNS PET MPO scores, and amenability to labeling with carbon-11 at a methyl group (Table 1).

We have previously reported the labeling of **L3** (NR2B-SMe) and its enantiomers in *S*-methyl position with carbon-11 for their evaluation as GluN2B radioligands in rat brain, as summarized in Scheme 7 [24]. Labeling was achieved readily by treating the methyl thiopropanoate precursor (**L19** or an enantiomer) with no-carrier-added [^{11}C]methyl iodide, produced rrom cyclotron-produced [^{11}C]carbon dioxide, as fully described in the Supporting Information of reference 24. No racemization occurred during the radiosyntheses from homochiral precursors, and therefore there was no need to use chiral chromatography for radioligand purification.

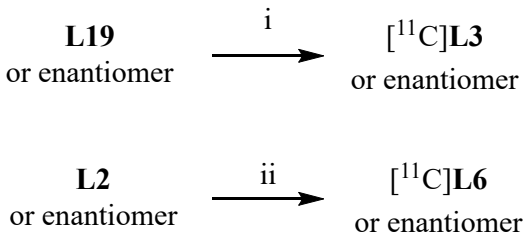

Scheme 7. Radiosyntheses of [^{11}C]**L3** and [^{11}C]**L6** and their enantiomers.

Reagents, conditions, and yields: (i) [^{11}C]Methyl iodide, 1 M TBAOH in MeOH; DMF, RT, 5 min. (15-20% for product formulated for i.v. injection from cyclotron-produced [^{11}C]carbon dioxide [24]. (ii) [^{11}C]Methyl iodide, CsF in MeOH, $Pd_2(dba)_3$, P(2,4-dimethylphenyl)$_3$, 80 ℃, 5 min; 20-30% for product formulated for i.v. injection from cyclotron-produced [^{11}C]carbon dioxide [25].

[^{11}C]**L6** ([^{11}C]NR2BMe) and its enantiomers have been labeled by palladium-mediated treatment of the boronic ester precursor **L21** or enantiomer with [^{11}C]methyl iodide (Scheme 7b), as fully described in the Supporting Information of reference 25. Again, no racemization occurred during the radiosyntheses from homochiral precursors,

PET radioligand performance. Both enantiomers of [^{11}C]**L3** performed well as radioligands for PET imaging in rats [24]. [^{11}C](*S*)-**L3** demonstrated high initial brain uptake, specific binding (up to 90% blockable), absence of radiometabolites in brain, and favorable characteristics for further evaluation in higher species. [^{11}C](*R*)-**L3** showed similar behavior, albeit with slightly faster washout characteristics.

[^{11}C]**L6** ([^{11}C]NR2BMe) and its enantiomers also entered rat brain avidly to give receptor-specific signals that were uncontaminated by radiometabolites. Unexpectedly high binding was seen in cerebellum with these radioligands, as for all others radioligands reported for PET imaging of GluN2B. This binding was determined not to be off-site binding to s_1 receptors [25], consistent with in vitro measurements of the low binding affinities of **L6** and several related ligands from this study for s_1 and s_2 receptors (Supporting Information Table S2). Notably, [^{11}C](*R*)-**L6** demonstrated good

 doi:10.20944/preprints202604.0788.v2

uptake and high specific binding in rhesus monkey brain. [^{11}C](*R*)-**L6** exhibited favorable regional non-displaceable binding potential (specific to non-specific binding ratio; BP_{ND}) values of 2 to 3 in a head-to-head comparison with previously reported radioligands, including [^{18}F]OF-Me-NB1 and [^{18}F]OF-NB1 [26].

Conclusions

In this study, we designed, synthesized, and evaluated a series of 3-alkylaryl derivatives of 7-methoxy-2,3,4,5-tetrahydro-1*H*-benzo[*d*]azepin-1-ol as ligands for the GluN2B subunit of the NMDA receptor. Systematic structural variation revealed that binding affinity is governed primarily by linker length, with a flexible four-carbon tether providing optimal positioning within the binding site, while the terminal aryl group is broadly tolerant to electronic and steric modification. The lack of correlation between affinity and lipophilicity further indicates that productive binding is driven by specific spatial and local interactions rather than global physicochemical properties. GluN2B binding affinity showed sensitivity to ligand absolute configuration, as explicable in docking studies.

From this series, ligands **L3** and **L6**, together with their enantiomers, emerged as promising candidates for PET radiotracer development, combining nanomolar affinity, favorable properties for brain imaging, and compatibility with carbon-11 labeling. Radiolabeled analogues demonstrated strong and specific binding in vivo, supporting their suitability for further translational evaluation.

Overall, these findings define key structure–activity relationships for this scaffold and establish 3-substituted 7-methoxy benzazepinols as a robust platform for the development of GluN2B PET radioligands.

Materials and Methods

Starting materials. 7-Methoxy-2,3,4,5-tetrahydro-1*H*-benzo[*d*]azepin-1-ol was obtained from Ambeed Inc. (Arlington Heights, Il). 4-Phenyl-1-butanol, 4-(4-methoxyphenyl)-1-butanol, 4-tolylbutan-1-ol, 4-(4-bromophenyl)butan-1-ol, 4-(4-fluorophenyl)butan-1-ol, 4-(*p*-iodophenyl)butyric acid, 3-butyn-1-ol, 5-hexyn-1-ol, 2-iodophenol, 4-iodobenzotrifluoride, diborane, triethylamine, bis(triphenylphosphine)palladium(II) dichloride, [1,1′-*bis*(diphenylphosphino)ferrocene]dichloropalladium(II)·CH_2Cl_2), and 4-(4-nitrophenyl)-1-butanol, were obtained from Aldrich (St Louis, MO). 2-Naphthalenebutanol was obtained from AstaTech (Bristol, PA). (Pyridin-2-yl)but-3-yn-1-ol, 2-bromo-6-fluoropyridine, 4-bromo-2-iodophenol, 4-fluoro-2-iodophenol, 2-iodo-4(trifluoromethyl)-phenol were obtained from Combi-Blocks (San Diego, CA).

Instruments and general methods .A microwave apparatus (Discover CP-D; CEM; Matthews, NC) was used for microwave-promoted reactions where indicated. A Combi-Flash apparatus (Teledyne Labs, Lincoln, NE) with a silica gel cartridge (4–80 g) was used in compound purifications, as later indicated. A Centrifan PE apparatus (Fisher Scientific; Waltham, MA) was used for drying many isolated compounds. Melting points were measured with a glass capillary on a digital melting point apparatus (SMP 20; Cole-Parmer Ltd, Stone, UK). Preparative, analytical, and chiral HPLC methods are detailed in Supporting Information (general methods A-F). Compound purities were calculated as area percentage of all chromatogram peaks. HRMS (ESI or EI) were acquired from Mass Spectrometry Lab (University of Illinois Urbana-Champaign, https://illinois.edu/). Optical rotation measurements were performed on a Jasco P-1010 Polarimeter.

LC-MS was performed on an Acquity UPLC M-Class System (Waters; Milford, MA), using a UPLC BEH column (1.7 mm, 2.1 × 50 mm) eluted at 0.4 mL/min with 0.1% formic acid in H_2O (A)/0.1% formic acid in acetonitrile (B) (B from 5 to 90% over 7 min).

^{1} H-NMR spectra were obtained at 400 MHz and ^{13}C-NMR spectra at 101 MHz at room temperature (RT) on a multinuclear instrument (Bruker Biospin) in deuterated solvent. TMS (δ = 0 ppm) was used as an internal standard for ^{1}H and ^{13}C-NMR spectroscopy. The abbreviations s, d, t, m, q, quint, dd, dt, brs, vs, vt, and AB denote singlet, doublet, triplet, multiplet, quartet, quintet,

 doi:10.20944/preprints202604.0788.v2

double doublet, double triplet, broad singlet, virtual singlet, virtual triplet, and AB coupling, respectively.

Chemistry

Syntheses of Tosylates T1–T18

4-Phenylbutyl 4-methylbenzenesulfonate (T1). 4-Phenylbutan-1-ol (6.5 mL, d = 0.984 g/mL, 42.6 mmol), tosyl chloride (15.11 g, 79.3 mmol), and Et_3N (21 mL, 151 mmol) were dissolved in DCM (100 mL) and stirred at RT overnight. A saturated sodium bicarbonate solution (200 mL) was added and then extracted with DCM. The organic layer was dried ($MgSO_4$), filtered, and then added to silica gel (60 mL). The solvent was removed under vacuum. The residue was purified (Combi-Flash, silica gel, hexane/ethyl acetate) to give **TI** as a colorless wax (10.0 g, yield 77%). ^{1}H-NMR ($CDCl_3$): δ 7.78 (d, $^3J_{HH}$ = 12 Hz, 2H, Ar-*H*), 7.33 (d, $^3J_{HH}$ = 8.0 Hz, 2H, Ar-*H*), 7.26 (vt, $^3J_{HH}$ = 8.0 Hz, 2H, Ar-*H*), 7.17 (t, $^3J_{HH}$ = 8.0 Hz, 1H, Ar-*H*), 7.10 (d, $^3J_{HH}$ = 8.0 Hz, 2H, Ar-*H*), 4.04 (t, $^3J_{HH}$ = 6.0 Hz, 2H, CH_2O), 2.56 (t, $^3J_{HH}$ = 6.0 Hz, 2H, CH_2), 2.45 (s, 3H, CH_3), 1.66 (m, 4H, CH_2CH_2). ^{13}C{^{1}H}-NMR ($CDCl_3$): δ 144.88, 141.75, 133.35, 130.02 (*C*H), 128.54 (*C*H), 128.06 (*C*H), 126.10 (*C*H), 70.58 (*C*H$_2$O), 35.26, 28.51, 27.26, 21.82 (*C*H$_3$). HRMS calcd for $C_{17}H_{24}NO_3$ [M + NH_4]$^+$: m/z = 322.1477, found 322.1476; error: –0.3 ppm.

4-(4-Iodophenyl)butyl 4-methylbenzenesulfonate (T2). Compound **1** (1.20 g, 4.35 mmol), tosyl chloride (1.07 g, 5.61 mmol), and Et_3N (2.0 mL, 14.3 mmol) were dissolved in DCM (20 mL) and stirred at RT for 24 h. Reaction progress was monitored with reversed phase HPLC (general method B). Silica gel (25 mL) was added and the solvent removed under vacuum. The residue was purified (Combi-Flash, silica gel, hexane/ethyl acetate) to give **T2** as white crystals (1.13 g. yield 61%). Mp: 58–60 °C. ^{1}H-NMR ($CDCl_3$): δ 7.77 (d, $^3J_{HH}$ = 8.2 Hz, 2H, Ar-*H*), 7.57 (d, $^3J_{HH}$ = 8.2 Hz, 2H, Ar-*H*), 7.33 (d, $^3J_{HH}$ = 8.1 Hz, 2H, Ar-*H*), 6.86 (d, $^3J_{HH}$ = 8.2 Hz, 2H, Ar-*H*), 4.03 (t, $^3J_{HH}$ = 5.8 Hz, 2H, CH_2O), 2.51 (t, $^3J_{HH}$ = 5.8 Hz, 2H, CH_2O), 2.45 (s, 3H, CH_3), 1.63–1.61 (m, 4H, CH_2CH_2). ^{13}C{^{1}H}-NMR ($CDCl_3$): δ 144.96, 141.38, 137.61 (*C*H), 133.32, 130.67 (*C*H), 130.05 (*C*H), 128.08 (*C*H), 91.15, 70.42 (*C*H$_2$O), 34.78, 28.45, 27.11, 21.86 (*C*H$_3$). HRMS calcd for $C_{17}H_{23}NO_3SI$ [M + NH_4]$^+$: m/z = 448.0443, found 448.0441; error: –0.4 ppm.

4-(4-(Methylthio)phenyl)butyl 4-methylbenzenesulfonate (T3). Compound **2** (0.51 g, 2.60 mmol), tosyl chloride (0.56 g, 2.94 mmol), and Et_3N (2.1 mL, 15.0 mmol) were dissolved in DCM (20 mL) and stirred at RT for 24 h. Reaction progress was monitored with reversed phase HPLC (general method B). Silica gel (10 mL) then was added and the solvent removed under vacuum. The residue was purified (Combi-Flash, silica gel, hexane/ethyl acetate) to give **T3** as a colorless oil (0.43 g, yield 47%). ^{1}H-NMR ($CDCl_3$): δ 7.77 (d, $^3J_{HH}$ = 12 Hz, 2H, Ar-*H*), 7.33 (d, $^3J_{HH}$ = 8.0 Hz, 2H, Ar-*H*), 7.17 (d, $^3J_{HH}$ = 8.0 Hz, 2H, Ar-*H*), 7.03 (d, $^3J_{HH}$ = 12 Hz, 2H, Ar-*H*), 4.03 (t, $^3J_{HH}$ = 6.0 Hz, 2H, CH_2O), 2.52 (t, $^3J_{HH}$ = 6.0 Hz, 2H, CH_2), 2.46 (s, 3H, CH_3), 2.44 (s, 3H, CH_3), 1.64 (m, 4H, CH_2CH_2). ^{13}C{^{1}H}-NMR ($CDCl_3$): δ 144.91, 138.88, 135.70, 133.38, 130.04, 129.11, 128.09, 127.34, 70.54 (*C*H$_2$O), 34.73, 28.49, 27.27, 21.86 (*C*H$_3$), 16.51 (S*C*H$_3$). HRMS calcd for $C_{18}H_{26}NO_3S_2$ [M + NH_4]$^+$: m/z = 368.1354, found 368.1348; error: –1.6 ppm.

4-(4-(Trifluoromethyl)phenyl)butyl 4-methylbenzenesulfonate (T4). Use of the method for **T3** in same molar proportions to **5** (1.0 g, 4.58 mmol) gave **T4** as white crystals (1.26 g, yield 74%). Mp: 52–54 °C. ^{1}H-NMR ($CDCl_3$): δ 7.78 (d, $^3J_{HH}$ = 8.0 Hz, 2H, Ar-*H*), 7.51 (d, $^3J_{HH}$ = 8.0 Hz, 2H, Ar-*H*), 7.33 (d, $^3J_{HH}$ = 8.0 Hz, 2H, Ar-*H*), 7.22 (d, $^3J_{HH}$ = 8.0 Hz, 2H, Ar-*H*), 4.04 (d, $^3J_{HH}$ = 6.0 Hz, 2H, CH_2), 2.65 (d, $^3J_{HH}$ = 6.0 Hz, 2H, CH_2), 1.68 (m, 4H, CH_2CH_2). ^{13}C{^{1}H}-NMR ($CDCl_3$): δ 145.87, 144.99, 133.31, 130.05, 128.85, 128.55 ($^2J_{CF}$ = 32.2 Hz), 128.07, 125.50 ($^3J_{CF}$ = 4.0 Hz), 124.51 ($^1J_{CF}$ = 272.7 Hz), 70.33 (*C*H$_2$O), 35.11, 28.49, 27.06, 21.82 (*C*H$_3$). HRMS calcd for $C_{18}H_{23}NO_3SF_3$ [M + NH_4]$^+$: m/z = 390.1351, found 390.1347; error: –1.0 ppm.

4-(4-Methoxyphenyl)butyl 4-methylbenzenesulfonate (T5). Use of the method for **T3** in the same molar proportions to 4-(4-methoxyphenyl)butan-1-ol (1.0 g, 5.5 mmol) gave **T5** as a pale -yellow oil (0.39 g, yield 21%). ^{1}H-NMR ($CDCl_3$): δ 7.77 (d, $^3J_{HH}$ = 8.1 Hz, 2H, Ar-*H*), 7.33 (d, $^3J_{HH}$ = 8.0 Hz, 2H, Ar-*H*), 7.01 (d, $^3J_{HH}$ = 8.4 Hz, 2H, Ar-*H*), 7.28 (d, $^3J_{HH}$ = 8.5 Hz, 2H, Ar-*H*), 4.03 (t, $^3J_{HH}$ = 6.0 Hz, 2H, CH_2), 3.78 (s, 3H, OCH_3), 2.50 (t, $^3J_{HH}$ = 6.0 Hz, 2H, CH_2), 2.44 (s, CH_3), 1.65–1.58 (m, 4H, CH_2CH_2).

 doi:10.20944/preprints202604.0788.v2

$^{13}C\{^{1}H\}$-NMR ($CDCl_3$): δ 158.03, 144.87, 133.82, 133.38, 130.01 (*C*H), 129.42 (*C*H), 128.07 (*C*H), 113.96 (*C*H), 70.63 (CH_2O), 55.45 (OCH_3), 34.35, 28.47, 27.49, 21.83 (CH_3). HRMS calcd for $C_{18}H_{26}NO_4S$ [*M* + NH_4]$^+$: *m*/*z* = 352.1583, found 352.1581; error: –0.6 ppm.

4-(*p*-Tolyl)butyl 4-methylbenzenesulfonate (T6). Use of the method for **T3** in the same molar proportions to 4-(*p*-tolyl)butan-1-ol (1.0 g, 6.1 mmol) gave **T6** as a colorless wax (0.46 g, yield 24%). ^{1}H-NMR ($CDCl_3$): δ 7.78 (d, $^{3}J_{HH}$ = 8.0 Hz, 2H, Ar-*H*), 7.33 (d, $^{3}J_{HH}$ = 8.0 Hz, 2H, Ar-*H*), 7.07 (d, $^{3}J_{HH}$ = 8.0 Hz, 2H, Ar-*H*), 6.99 (d, $^{3}J_{HH}$ = 8.0 Hz, 2H, Ar-*H*), 4.03 (t, $^{3}J_{HH}$ = 6.0 Hz, 2H, CH_2O), 2.52 (t, $^{3}J_{HH}$ = 6.0 Hz, 2H, CH_2), 2.44 (s, 3H, CH_3), 2.31 (s, 3H, CH_3), 1.66–1.61 (m, 4H, CH_2CH_2). $^{13}C\{^{1}H\}$-NMR ($CDCl_3$): δ 144.87, 138.67, 135.57, 133.40, 130.02 (*C*H), 129.24 (*C*H), 128.43 (*C*H), 128.09 (*C*H), 70.63 (CH_2O), 34.83, 28.53, 27.38, 21.85 (CH_3), 21.19 (CH_3). HRMS calcd for $C_{18}H_{26}NO_3S$ [*M* + NH_4]$^+$: *m*/*z* = 336.1633, found 366.1633; error: 0.0 ppm.

4-(4-Bromophenyl)butyl 4-methylbenzenesulfonate (T7). 4-(4-Bromophenyl)butan-1-ol (1.0 g, 4.4 mmol), tosyl chloride (0.99 g, 5.2 mmol) and Et_3N (2 mL, 14.3 mmol) were dissolved in DCM (20 mL). The reaction mixture was stirred at RT for 5 d. Reaction progress was monitored with HPLC (general method A). Silica gel (60 mL) was then added and the solvent removed under vacuum. The residue was then purified (Combi-Flash, silica gel, hexane/ethyl acetate) to give **T7** as a pale-yellow wax (0.97 g, yield 58%). ^{1}H-NMR ($CDCl_3$): δ 7.77 (d, $^{3}J_{HH}$ = 8.0 Hz, 2H, Ar-*H*), 7.36 (d, $^{3}J_{HH}$ = 8.0 Hz, 2H, Ar-*H*), 7.33 (d, $^{3}J_{HH}$ = 8.0 Hz, 2H, Ar-*H*), 6.97 (d, $^{3}J_{HH}$ = 8.0 Hz, 2H, Ar-*H*), 4.02 (t, $^{3}J_{HH}$ = 6.0 Hz, 2H, CH_2O), 2.51 (t, $^{3}J_{HH}$ = 6.0 Hz, 2H, CH_2), 2.44 (s, 3H, CH_3), 1.64–1.62 (m, 4H, CH_2CH_2). $^{13}C\{^{1}H\}$-NMR ($CDCl_3$): δ 144.93, 140.68, 133.27, 131.56 (*C*H), 130.28 (*C*H), 130.01 (Ts, *C*H), 128.02 (Ts, *C*H), 119.80, 70.40 (CH_2O), 34.63, 28.40, 27.10, 21.81 (CH_3). HRMS calcd for $C_{17}H_{23}NO_3SBr$ [*M* + NH_4]$^+$: *m*/*z* = 400.0582, found 400.0588; error: 1.5 ppm.

4-(4-Fluorophenyl)butyl 4-methylbenzenesulfonate (T8). 4-(4-Fluorophenyl)butan-1-ol (1.0 g, 4.4 mmol), tosyl chloride (1.22 g, 6.4 mmol), and Et_3N (2.5 mL, *d* = 0.726 g/mL, 17.9 mmol) were dissolved in DCM (20 mL). The reaction mixture was stirred at RT for 5 d. Silica gel (20 mL) was then added and the solvent was removed under vacuum. The residue was then purified (Combi-Flash, silica gel, hexane/ethyl acetate) to give **T8** as a colorless oil (0.99 g. yield 52%). ^{1}H-NMR ($CDCl_3$): δ 7.78 (d, $^{3}J_{HH}$ = 12.0 Hz, 2H, Ar-H), 7.33 (d, $^{3}J_{HH}$ = 8.0 Hz, 2H, Ar-*H*), 7.06 (dd, $^{3}J_{HH}$ = 8.0 Hz, $^{3}J_{HF}$ = 4.0 Hz, 2H, Ar-*H*), 6.94 (t, $^{3}J_{HH}$ = 8.0 Hz, 2H, Ar-*H*), 4.03 (t, $^{3}J_{HH}$ = 6.0 Hz, 2H, CH_2), 2.54 (t, $^{3}J_{HH}$ = 6.0 Hz, 2H, CH_2), 2.44 (s, CH_3), 1.64 (m, 4H, CH_2CH_2). $^{13}C\{^{1}H\}$-NMR ($CDCl_3$): δ 161.49 (d, $^{1}J_{CF}$ = 243.5 Hz, Fph, *C*-F), 144.92, 137.6 (d, $^{4}J_{CF}$ = 3.0 Hz, Fph, *C*HCHCHCF), 133.35, 130.03 (*C*H), 129.85 (d, $^{3}J_{CF}$ = 8.0 Hz, Fph, *C*HCHCF), 128.07 (*C*H), 115.29 (d, $^{2}J_{CF}$ = 21.1 Hz, Fph, *C*HCF), 70.49 (CH_2O), 34.47, 28.46, 27.42, 21.83 (CH_3). HRMS calcd for $C_{17}H_{23}NO_3SF$ [*M* + NH_4]$^+$: *m*/*z* = 340.1383, found 340.1378; error: –1.5 ppm.

4-(Naphthalen-2-yl)butyl 4-methylbenzenesulfonate (T9). Use of the method for **T8** in the same molar proportions to 4-(naphthalen-2-yl)butan-1-ol (1.0 g, 5.0 mmol) gave **T9** as tan crystals (0.39 g, yield 22%). Mp: 34–36 °C). ^{1}H-NMR ($CDCl_3$): δ 7.81–7.75 (m, 5H, Ar-*H*), 7.54 (s, 1H, Ar-*H*), 7.46 (t, $^{3}J_{HH}$ = 6.5 Hz, 1H, Ar-*H*), 7.42 (t, $^{3}J_{HH}$ = 6.5 Hz, 1H, Ar-*H*), 7.30 (d, $^{3}J_{HH}$ = 8.0 Hz, 2H, Ts, Ts-*H*), 7.26 (d, $^{3}J_{HH}$ = 8.3 Hz, 1H, Np-*H*), 4.06 (t, $^{3}J_{HH}$ = 5.8 Hz, 2H, CH_2), 2.74 (t, $^{3}J_{HH}$ = 5.8 Hz, 2H, CH_2), 2.42 (s, CH_3), 1.75–1.70 (m, 4H, CH_2CH_2). $^{13}C\{^{1}H\}$-NMR ($CDCl_3$): δ 144.87, 139.24, 133.75, 133.34, 132.22, 130.01 (Ts, *C*H), 128.14 (*C*H), 128.06 (Ts, *C*H), 127.80 (*C*H), 127.58 (*C*H), 127.32 (*C*H), 126.63 (*C*H), 126.16 (*C*H), 125.42 (*C*H), 70.59 (CH_2O), 35.40, 28.52, 27.13, 21.80 (CH_3). HRMS calcd for $C_{21}H_{26}NO_3S$ [*M* + NH_4]$^+$: *m*/*z* = 372.1633, found 372.1638; error: 1.3 ppm.

4-(Pyridin-2-yl)butyl 4-methylbenzenesulfonate (T10). 4-(Pyridin-2-yl)butan-1-ol (5.0 g, 33.1 mmol), tosyl chloride (7.66 g, 40.2 mmol), and Et_3N (12 mL, 86.1 mmol) were dissolved in ethyl acetate (100 mL). The reaction mixture was stirred at RT for 24 h. Reaction progress was monitored with HPLC. Silica gel (60 mL) was then added and the solvent removed under vacuum. The residue was purified (Combi-Flash, silica gel, hexane/ethyl acetate) to give **T10** as a thick colorless oil (2.09 g, yield 21%). ^{1}H-NMR ($CDCl_3$): δ 8.42 (d, $^{3}J_{HH}$ = 4.0 Hz, 1H, py-*H*), 8.36 (s, 1H, py-*H*), 7.76 (d, $^{3}J_{HH}$ = 12.0 Hz, 2H, Ts-*H*), 7.42 (d, $^{3}J_{HH}$ = 8.0 Hz, 1H, py-*H*), 7.32 (d, $^{3}J_{HH}$ = 12.0 Hz, 2H, Ts-*H*), 7.18 (dd, $^{3}J_{HH}$ = 8.0 Hz, $^{3}J_{HH}$ = 4.0 Hz, 1H, py-*H*), 4.02 (t, $^{3}J_{HH}$ = 6.0 Hz, 2H, CH_2), 2.55 (t, $^{3}J_{HH}$ = 6.0 Hz, 2H, CH_2), 2.42 (s, 3H, CH_3), 1.66–1.64 (m, 4H, CH_2CH_2). $^{13}C\{^{1}H\}$-NMR ($CDCl_3$): δ 149.99 (*C*H), 147.70 (*C*H), 144.96, 136.88,

 doi:10.20944/preprints202604.0788.v2

135.85 (*C*H), 133.18, 130.00 (Ts, *C*H), 127.99 (Ts, *C*H), 123.46, 70.22 (*C*H$_2$O), 32.34, 28.40, 27.00, 21.77 (*C*H$_3$). HRMS calcd for $C_7H_7O_3S^-$: *m*/*z* = 171.0116, found 171.0119. Error (ppm): 1.8. HRMS calcd for $C_9H_{12}N^+$: *m*/*z* = 134.0970, found 134.0967; error: –2.2 ppm.

4-(Pyridin-2-yl)but-3-yn-1-yl 4-methylbenzenesulfonate (T11). 4-(Pyridin-2-yl)but-3-yn-1-ol (1.99 g, 13.5 mmol), tosyl chloride (3.11 g, 16.3 mmol), and Et$_3$N (6.0 mL, 43.0 mmol) were dissolved in DCM (100 mL). The reaction mixture was stirred at RT for 24 h. Reaction progress was monitored with HPLC (general method B). Silica gel (60 mL) was then added and the solvent removed under vacuum. The residue was purified (Combi-Flash, silica gel, hexane/ethyl acetate) to give **T11** as a clear wax (0.88 g, yield 22%). ^{1}H-NMR (CDCl$_3$): δ 8.54 (d, $^3J_{HH}$ = 8.0 Hz, 1H, py-*H*), 7.82 (d, $^3J_{HH}$ = 8.0 Hz, 2H, Ts-*H*), 7.63 (dt, $^3J_{HH}$ = 8.0 Hz, $^4J_{HH}$ = 2.0 Hz, 1H, py-*H*), 7.34 (d, $^3J_{HH}$ = 8.0 Hz, 1H, py-*H*), 7.32 (d, $^3J_{HH}$ = 8.0 Hz, 2H, Ts-*H*), 7.21 (dd, $^3J_{HH}$ = 8.0 Hz, $^3J_{HH}$ = 4.0 Hz, 1H, py-*H*), 4.20 (t, $^3J_{HH}$ = 6.0 Hz, 2H, C*H*$_2$), 2.82 (t, $^3J_{HH}$ = 6.0 Hz, 2H, C*H*$_2$), 2.43 (s, 3H, C*H*$_3$). ^{13}C{^{1}H}-NMR (CDCl$_3$): δ 150.13 (py, *C*H), 145.21, 143.20, 136.33 (py, *C*H), 132.98, 130.13 (Ts, *C*H), 128.22 (Ts, *C*H), 127.20 (py, *C*H), 123.08 (py, *C*H), 84.36 (*C*2), 82.48 (*C*2), 67.49 (*C*H$_2$O), 21.86 (*C*H$_3$), 20.50. HRMS calcd for $C_{16}H_{16}NO_3S$ [*M* + H]$^+$: *m*/*z* = 302.0851, found 302.0854; error: 1.0 ppm.

4-(6-Fluoropyridin-2-yl)but-3-yn-1-yl 4-methylbenzenesulfonate (T12). 4-(6-Fluoropyridin-2-yl)but-3-yn-1-ol (**3**, 2.65 g, 16.0 mmol), tosyl chloride (3.18 g, 16.7 mmol), and Et$_3$N (10 mL, *d* = 0.726 g/mL, 71.7 mmol) were dissolved in DCM (40 mL). The reaction mixture was stirred at RT for 24 h. Reaction progress was monitored with HPLC (general method B). Silica gel (60 mL) was added and the solvent removed under vacuum. The reaction mixture was then purified (Combi-Flash, silica gel, hexane/ethyl acetate) to give **T12** as a clear wax (0.68 g, yield 13%). ^{1}H-NMR (CDCl$_3$): δ 7.82 (d, $^3J_{HH}$ = 8.1 Hz, 2H, Ar-*H*), 7.73 (pseudo-q, $^3J_{HH}$ = $^3J_{HF}$ = 7.9 Hz, 1H, Ar-*H*), 7.34 (d, $^3J_{HH}$ = 8.0 Hz, 2H, Ar-*H*), 7.23 (dd, $^3J_{HH}$ = 7.4 Hz, $^5J_{HF}$ = 1.9 Hz, 1H, Ar-*H*), 6.88 (dd, $^3J_{HH}$ = 8.3 Hz, $^3J_{HF}$ = 2.7 Hz, 1H, Ar-*H*), 4.19 (t, $^3J_{HH}$ = 6.0 Hz, 2H, C*H*$_2$), 2.81 (t, $^3J_{HH}$ = 6.0 Hz, 2H, C*H*$_2$), 2.44 (s, C*H*$_3$). ^{13}C{^{1}H}-NMR (CDCl$_3$): δ 163.1 (d, $^1J_{CF}$ = 250 Hz), 145.28, 141.38 (d, J_{CF} = 8.1 Hz), 141.25 (d, J_{CF} = 37.5 Hz), 132.93, 130.18 (Ts, *C*H), 128.22 (Ts, *C*H), 124.69 (d, J_{CF} = 4.0 Hz), 109.66 (d, $^1J_{CF}$ = 36.6 Hz), 85.87 (*C*$_2$), 81.23 (*C*$_2$), 67.28 (*C*H$_2$O), 21.86, 20.50 (*C*H$_3$). HRMS calcd for $C_{16}H_{15}NO_3FS$ [*M* + H]$^+$: *m*/*z* = 320.0757, found 320.0763; error: 1.9 ppm.

2-(Benzofuran-2-yl)ethyl 4-methylbenzenesulfonate (T13). Use of the method for **T12** in the same molar proportions to **6** (910 mg, 5.61 mmol) gave **T13** as white crystals (799 mg, yield 45%). Mp: 76–77 °C. ^{1}H-NMR (CDCl$_3$): δ 7.67 (d, $^3J_{HH}$ = 8.0 Hz, 2H, Ts, Ar-*H*), 7.46 (d, $^3J_{HH}$ = 7.3 Hz, 1H, BFu, Ar-*H*), 7.30 (d, $^3J_{HH}$ = 7.7 Hz, 1H, BFu, Ar-*H*,), 7.24–7.18 (m, 2H, BFu Ar-*H*), 7.17 (d, $^3J_{HH}$ = 8.0 Hz, 2H, Ts, Ar-*H*), 6.42 (s, 1H, BFu, Ar-*H*), 4.36 (t, $^3J_{HH}$ = 6.3 Hz, 2H, C*H*$_2$), 3.12 (t, $^3J_{HH}$ = 6.3 Hz, 2H, C*H*$_2$), 2.37 (s, 3H, C*H*$_3$). ^{13}C{^{1}H}-NMR (CDCl$_3$): δ 154.90, 153.29, 144.98, 132.83, 129.92 (Ts, *C*H), 128.64, 127.99 (Ts, *C*H), 123.92 (BFu, *C*H), 122.87 (BFu, *C*H), 120.77 (BFu, *C*H), 111.02 (BFu, *C*H), 104.54 (BFu, *C*H), 67.55 (*C*H$_2$O), 28.75 (*C*H$_2$), 21.81 (*C*H$_3$). HRMS calcd for $C_{17}H_{20}NO_4S$ [*M* + NH$_4$]$^+$: *m*/*z* = 334.1113, found 334.1114; error: 0.3 ppm.

2-(5-Bromobenzofuran-2-yl)ethyl 4-methylbenzenesulfonate (T14). Use of the method for **T12** in the same molar proportions to **7** (790 mg, 3.28 mmol) gave **T14** as white crystals (699 mg, yield 54%). Mp: 88–90 °C. ^{1}H-NMR (CDCl$_3$): δ 7.67 (d, $^3J_{HH}$ = 8.0 Hz, 2H, Ts, Ar-*H*), 7.58 (s, 1H, BFu, Ar-*H*), 7.31 (d, $^3J_{HH}$ = 8.7 Hz, 1H, BFu, Ar-*H*), 7.18 (d, $^3J_{HH}$ = 8.0 Hz, $^3J_{HH}$ = 8.7 Hz, 3H, BFu-Ts, Ar-*H*), 6.36 (s, 1H, BFu, Ar-*H*), 4.36 (t, $^3J_{HH}$ = 6.3 Hz, 2H, CH$_2$), 3.11 (t, $^3J_{HH}$ = 6.3 Hz, 2H, C*H*$_2$), 2.38 (s, 3H, C*H*$_3$). ^{13}C{^{1}H}-NMR (CDCl$_3$): δ 154.91, 153.65, 145.06, 132.84, 130.64, 129.93 (Ts, *C*H), 127.97 (Ts, *C*H), 126.82 (BFu, CH), 123.44 (BFu, *C*H), 115.93, 112.48 (BFu, *C*H), 104.10 (BFu, *C*H), 67.32 (*C*H$_2$O), 28.76 (*C*H$_2$), 21.83 (*C*H$_3$). HRMS calcd for $C_{17}H_{19}NO_4SBr$ [*M* + NH$_4$]$^+$: *m*/*z* = 412.0218, found 412.0225; error: 1.7 ppm.

2-(5-Fluorobenzofuran-2-yl)ethyl 4-methylbenzenesulfonate (T15). Use of the method for **T12** in the same molar proportions to **8** (610 mg, 3.39 mmol) gave **T15** as white crystals (815 mg, yield 72%). Mp: 76–78 °C. ^{1}H-NMR (CDCl$_3$): δ 7.68 (d, $^3J_{HH}$ = 8.1 Hz, 2H, Ts, Ar-*H*), 7.23 (dd, $^3J_{HF}$ = 4.1 Hz, $^3J_{HH}$ = 8.9 Hz, 1H, BFu), 7.20 (d, $^3J_{HH}$ = 8.1 Hz, 2H, Ts, Ar-*H*), 7.11 (dd, $^4J_{HF}$ = 2.5 Hz, $^3J_{HH}$ = 9.0 Hz, 1H, BFu, Ar-*H*), 6.93 (td, $^3J_{HF}$ = $^4J_{HH}$ = 8.6 Hz, $^4J_{HH}$ = 2.5 Hz, 1H, BFu, Ar-*H*), 6.40 (s, 1H), 4.36 (t, $^3J_{HH}$ = 6.4 Hz, 2H, C*H*$_2$), 3.11 (t, $^3J_{HH}$ = 6.4 Hz, 2H, C*H*$_2$), 2.38 (s, 3H, C*H*$_3$). ^{13}C{^{1}H}-NMR (CDCl$_3$): δ 154.35 (d, $^1J_{CF}$ = 236.4 Hz), 155.32, 151.13, 145.04, 132.87, 129.94 (Ts, *C*H), 129.45 (d, J_{CF} = 10.8 Hz, *C*H), 128.01 (Ts,

 doi:10.20944/preprints202604.0788.v2

*C*H), 111.64 (d, J_{CF} = 2.7 Hz, *C*H), 111.46 (d, J_{CF} = 13.8 Hz, *C*H), 106.35 (d, J_{CF} = 25.0 Hz, *C*H), 104.81 (d, J_{CF} = 4.0 Hz, *C*H), 67.37 (*C*H$_2$O), 28.84 (*C*H$_2$), 21.82 (*C*H$_3$). HRMS calcd for $C_{17}H_{19}NO_4FS$ [*M* + NH$_4$]$^+$: *m*/*z* = 352.1019, found 352.1017; error:–0.6 ppm.

2-(5-Trifluoromethylbenzofuran-2-yl)ethyl 4-methylbenzenesulfonate (T16). Use of the method for **T12** in the same molar proportions to **9** (1.07 g, 4.65 mmol) gave **T16** as white crystals (697 mg, yield 39%). Mp: 94–95 °C. ^{1}H-NMR (CD$_3$OD): *δ* 7.74 (s, 1H, Ar-*H*), 7.53 (dd, $^3J_{HH}$ = 6.6 Hz, $^4J_{HH}$ = 1.6 Hz, 2H, Ar-*H*), 7.44 (AB, $^3J_{HH}$ = 8.7 Hz, $^4J_{HH}$ = 1.7 Hz, 1H, Ar-*H*), 7.40 (AB, $^4J_{HH}$ = 8.7 Hz, 1H, Ar-*H*), 7.09 (d, $^3J_{HH}$ = 8.0 Hz, 2H, Ar-*H*), 6.52 (d, $^4J_{HH}$ = 0.7 Hz, 1H, Ar-*H*), 4.32 (t, $^3J_{HH}$ = 5.7 Hz, 2H, C*H*$_2$), 3.07 (t, $^3J_{HH}$ = 5.7 Hz, 2H, C*H*$_2$), 2.24 (s, 3H, Ar-C*H*$_3$). ^{13}C{^{1}H}-NMR (CD$_3$OD): *δ* 157.93, 157.68, 146.47, 134.19, 130.96 (Ts, *C*H), 130.44, 128.95 (Ts, *C*H), 126.37 (q, $^1J_{CF}$ = 271.0 Hz, 1C, *C*F), 126.51 (q, $^2J_{CF}$ = 32.0 Hz, 1C), 122.06 (q, $^3J_{CF}$ = 3.6 Hz, 1C, BFu, *C*H), 119.38 (q, $^3J_{CF}$ = 4.3 Hz, 1C, BFu *C*H), 112.58 (BFu, *C*H), 105.70 (BFu, *C*H), 69.02, (*C*H$_2$O), 29.40 (*C*H$_2$), 21.66 (*C*H$_3$). HRMS calcd for $C_{18}H_{19}NO_4F_3S$ [*M* + NH$_4$]$^+$: *m*/*z* = 402.0987, found 402.0992; error: 1.2 ppm.

4-(Benzofuran-2-yl)butyl 4-methylbenzenesulfonate (T17). Use of the method for **T12** in the same molar proportions to **10** (710 mg, 3.73 mmol) gave **T17** as a clear wax (977 mg, yield 76%). ^{1}H-NMR (CDCl$_3$): *δ* 7.78 (d, $^3J_{HH}$ = 8.0 Hz, 2H, Ts, Ar-*H*), 7.47 (d, $^3J_{HH}$ = 7.4 Hz, 1H, BFu, Ar-*H*), 7.39 (d, $^3J_{HH}$ = 7.6 Hz, 1H, BFu, Ar-*H*), 7.32 (d, $^3J_{HH}$ = 8.0 Hz, 2H, Ts, Ar-*H*), 7.21–7.17 (m, 2H, BFu, Ar-*H*), 6.34 (s, 1H, BFu, Ar-*H*), 4.07 (t, $^3J_{HH}$ = 5.7 Hz, 2H, C*H*$_2$), 2.72 (t, $^3J_{HH}$ = 5.7 Hz, 2H, C*H*$_2$), 2.43 (s, 3H, C*H*$_3$), 1.76 (m, 4H, C*H*$_2$C*H*$_2$). ^{13}C{^{1}H}-NMR (CDCl$_3$): *δ* 158.49, 154.83, 144.95, 132.83, 130.05 (Ts, *C*H), 128.98, 128.08 (Ts, *C*H), 123.48 (BFu, *C*H), 122.69 (BFu, *C*H), 120.47 (BFu, *C*H), 111.93 (BFu, *C*H), 102.53 (BFu, *C*H), 70.29 (*C*H$_2$O), 28.41 (*C*H$_2$), 27.84 (*C*H$_2$), 23.82 (*C*H$_2$), 21.82 (*C*H$_3$). HRMS calcd for $C_{19}H_{24}NO_4S$ [*M* + NH$_4$]$^+$: *m*/*z* = 362.1426, found 362.1419; error: –1.9 ppm.

4-(5-(Trifluoromethyl)benzofuran-2-yl)butyl 4-methylbenzenesulfonate (T18). Use of the method for **T12** in the same molar proportions to **11** (425 mg, 1.65 mmol) gave **T18** as a clear wax (380 mg, yield 56%). ^{1}H-NMR (CDCl$_3$): *δ* 7.78 (d, $^3J_{HH}$ = 8.0 Hz, 2H, Ts-*H*), 7.76 (s, 1H, Ar-*H*), 7.49-7.45 (AB, $^3J_{HH}$ = 8.0 Hz, 2H, Ar-*H*), 7.32 (d, $^3J_{HH}$ = 8.0 Hz, 2H, Ts-*H*), 6.42 (s, 1H, Ar-*H*), 4.07 (t, $^3J_{HH}$ = 6.0 Hz, 2H, C*H*$_2$), 2.77 (t, $^3J_{HH}$ = 6.0 Hz, 2H, C*H*$_2$), 2.43 (s, 3H, C*H*$_3$), 1.83–1.61 (m, 4H, C*H*$_2$C*H*$_2$). ^{13}C{^{1}H}-NMR (CDCl$_3$): *δ* 160.62, 156.22, 145.02 (Ts), 133.26 (Ts), 130.06 (Ts, *C*H), 129.07, 128.08 (Ts, *C*H), 125.44 (q, $^2J_{CF}$ = 32 Hz), 124.93 (q, $^1J_{CF}$ = 271 Hz, *C*F$_3$), 120.72 (q, $^2J_{CF}$ = 3.0 Hz, *C*HCF), 110.13 (q, $^2J_{CF}$ = 4.0 Hz, *C*HCF), 70.14 (*C*H$_2$O), 28.43, 27.87, 23.73, 21.82. HRMS calcd for $C_{20}H_{23}NO_4F_3S$ [*M* + NH$_4$]$^+$: *m*/*z* = 430.1300, found 430.1305; error: 1.2 ppm.

Syntheses of Racemic GluN2B Ligands L1–L20

7-Methoxy-3-(4-(phenyl)butyl)-2,3,4,5-tetrahydro-1*H*-benzo[*d*]azepin-1-ol (L1). 7-Methoxy-2,3,4,5-tetrahydro-1*H*-benzo[*d*]azepin-1-ol (190 mg, 0.98 mmol), **T1** (390 mg, 1.28 mmol), and K$_2$CO$_3$ (610 mg, 4.4 mmol) were suspended in acetonitrile (10 mL) and refluxed for 6 d. Reaction progress was monitored with HPLC (general method A). The reaction mixture was cooled to RT, passed through a 0.2 µm syringe filter and then purified with HPLC (general method C). The solvent was then removed under vacuum. The residue was dissolved in acetonitrile, passed through a 0.2 µm syringe filter, and dried with Centrifan to give **L1** as white crystals (0.23 g, yield 72%). Mp: 78–79 °C. ^{1}H-NMR (CDCl$_3$): *δ* 7.28 (t, $^3J_{HH}$ = 8.0 Hz, 2H, *m*-Ar-*H*), 7.18 (t, $^3J_{HH}$ = 8.0 Hz, 1H, *p*-Ar-*H*), 7.18 (d, $^3J_{HH}$ = 8.0 Hz, 2H, *o*-Ar-*H*), 7.10 (d, $^3J_{HH}$ = 8.0 Hz, 1H, Ar-*H*), 6.64 (dd, $^3J_{HH}$ = 8.0 Hz, $^4J_{HH}$ = 4.0 Hz, 1H, Ar-*H*), 6.63 (brs, 1H, Ar-*H*), 4.59 (d, $^3J_{HH}$ = 4.0 Hz, 1H, C*H*-OH), 3.76 (s, 3H, OC*H*$_3$), 3.26 (vt, $^2J_{HH}$ = 12 Hz, 1H, C*H*$_2$), 3.18–3.14 (m, 1H, C*H*$_2$), 3.02–2.97 (m, 1H, C*H*$_2$), 2.68–2.59 (m, 5H, C*H*$_2$), 2.53 (d, $^2J_{HH}$ = 12 Hz, 1H, C*H*$_2$), 2.43 (vt, $^2J_{HH}$ = 12 Hz, 1H, C*H*$_2$), 1.69–1.62 (m, 2H, C*H*$_2$), 1.61–1.54 (m, 2H, C*H*$_2$). ^{13}C{^{1}H}-NMR (CDCl$_3$): *δ* 159.09, 142.43, 141.25, 135.57, 129.86, 128.57 (*C*H), 128.52 (*C*H), 125.97 (*C*H), 116.74 (*C*H), 110.39 (*C*H), 72.42 (*C*HO), 60.88 (*C*N), 59.76 (*C*N), 56.19 (*C*N), 55.38 (OC*H*$_3$), 36.52, 35.92, 29.28, 26.66. HRMS calcd for $C_{21}H_{28}NO_2$ [*M* + H]$^+$: *m*/*z* = 326.2120, found 326.2126; error: 1.8 ppm. HPLC (general method A): t_R = 5.14 min, purity 99.62%.

7-Methoxy-3-(4-(4-iodophenyl)butyl)-2,3,4,5-tetrahydro-1*H*-benzo[*d*]azepin-1-ol (L2). 7-Methoxy-2,3,4,5-tetrahydro-1*H*-benzo[*d*]azepin-1-ol (420 mg, 2.17 mmol), **T2** (1.13 g, 2.63 mmol), and

 doi:10.20944/preprints202604.0788.v2

Na_2HPO_4 (1.30 g, 9.2 mmol) were suspended in acetonitrile (8 mL) and heated at 75 °C for 5 d. Reaction progress was monitored with HPLC (general method A). The reaction mixture was then cooled to RT, passed through a 0.2 µm syringe filter, and purified with HPLC (general method C). The solvent was then removed under vacuum. The residue was dissolved in ethanol, passed through a 0.2 µm syringe filter, and dried with Centrifan to give **L2** as white crystals (0.714 g, yield 73%). Mp: 100–101 °C. ^{1}H-NMR ($CDCl_3$): δ 7.60 (d, $^3J_{HH}$ = 8.0 Hz, 2H, Ar-*H*), 7.16 (d, $^3J_{HH}$ = 8.0 Hz, 1H, Ar-*H*), 6.92 (d, $^3J_{HH}$ = 8.0 Hz, 2H, Ar-*H*), 6.69 (dd, $^3J_{HH}$ = 8.0 Hz, $^4J_{HH}$ = 4.0 Hz, 1H, Ar-*H*), 6.65 (d, $^4J_{HH}$ = 4.0 Hz, 1H, Ar-*H*), 4.76 (brs, 1H, C*H*OH), 3.78 (s, 3H, OCH_3), 3.39–3.32 (m, 2H, CH_2), 3.16–3.12 (m, 1H, CH_2), 2.75 (brs, 4H, CH_2), 2.60–2.58 (m, 3H, CH_2), 1.63 (m, 4H, CH_2). ^{13}C{^{1}H}-NMR ($CDCl_3$): δ 159.34, 141.60, 140.31, 137.64 (*C*H), 134.50, 130.67 (*C*H), 129.80, 116.62 (*C*H), 110.89 (*C*H), 91.16 (C_{Ar}–I), 71.47 (*C*HO), 60.33 (*C*N), 59.45 (*C*N), 55.79 (*C*N), 55.46 (O*C*H$_3$), 42.47, 35.20, 28.81, 25.46, 11.26. HRMS calcd for $C_{21}H_{27}INO_2$ [*M* + H]$^+$: *m*/*z* = 452.1086, found 452.1092; error: 1.3 ppm. HPLC (general method A): t_R = 7.31 min, purity 100%.

7-Methoxy-3-(4-(4-(methylthio)phenyl)butyl)-2,3,4,5-tetrahydro-1*H*-benzo[*d*]azepin-1-ol (L3). 7-Methoxy-2,3,4,5-tetrahydro-1*H*-benzo[*d*]azepin-1-ol (200 mg, 1.03 mmol), **T3** (450 mg, 1.28 mmol), and Na_2HPO_4 (620 mg, 4.4 mmol) were suspended in acetonitrile (2 mL) and heated at 75 °C for 2 d. Reaction progress was monitored with HPLC (general method A). The reaction mixture was cooled to RT, passed through a 0.2 µm syringe filter, and then purified with HPLC (general method C). The solvent was removed under vacuum. The residue was dissolved in ethanol and Na_2CO_3 (1.0 g, 9.4 mmol) was added. The mixture was sonicated for 5 min and then stirred at RT for 1 min before finally being passed through a 0.2 µm syringe filter and dried with a Centrifan to give **L3** as white crystals (0.288 g, yield 75%). Mp: 89–91 °C. ^{1}H-NMR ($CDCl_3$): δ 7.18 (AB, $^3J_{HH}$ = 8.0 Hz, 2H, Ar-*H*), 7.09 (AB, $^3J_{HH}$ = 8.0 Hz, 1H, Ar-*H*), 7.08 (d, $^3J_{HH}$ = 8.0 Hz, 1H, Ar-*H*), 6.63 (dd, $^3J_{HH}$ = 8.0 Hz, $^4J_{HH}$ = 4.0 Hz, 1H, Ar-*H*), 6.62 (brs, 1H, Ar-*H*), 4.56 (d, $^3J_{HH}$ = 4.0 Hz, 1H, C*H*OH), 3.75 (s, 3H, OCH_3), 3.25 (vt, $^2J_{HH}$ = 12 Hz, 1H, CH_2), 3.17–3.12 (m, 1H, CH_2), 3.00–2.95 (m, 1H, CH_2), 2.66–2.60 (m, 1H, CH_2), 2.58 (t, $^3J_{HH}$ = 8.0 Hz, 4H, CH_2), 2.50 (d, $^2J_{HH}$ = 12 Hz, 1H, CH_2), 2.45 (s, 3H, SCH_3), 2.39 (vt, $^2J_{HH}$ = 12 Hz, 1H, CH_2), 1.62 (quint, $^3J_{HH}$ = 8.0 Hz, 2H, CH_2), 1.54 (quint, $^3J_{HH}$ = 8.0 Hz, 2H, CH_2). ^{13}C{^{1}H}-NMR ($CDCl_3$): δ 159.14, 141.36, 139.64, 135.69, 135.45, 129.94, 129.15 (*C*H), 127.39 (*C*H), 116.82 (*C*H), 110.40 (*C*H), 72.60 (*C*HO), 60.97 (*C*N), 59.79 (*C*N), 56.31 (*C*N), 55.42 (OCH$_3$), 37.04, 35.40, 29.28, 26.77, 16.57 (SCH$_3$). HRMS calcd for $C_{22}H_{30}NO_2S$ [*M* + H]$^+$: *m*/*z* = 372.1997, found 372.1999; error: 0.51 ppm. HPLC (general method A): t_R = 7.31 min, purity 100%.

7-Methoxy-3-(4-(4-trifluoromethylphenyl)butyl)-2,3,4,5-tetrahydro-1*H*-benzo[*d*]azepin-1-ol (L4). Use of the method for **L3** in the same molar proportions to **t4** (240 mg, 0.64 mmol) gave **L4** as white crystals. (0.232 g, yield 71%). Mp: 79–81 °C. ^{1}H-NMR ($CDCl_3$): δ 7.52 (d, $^3J_{HH}$ = 8.0 Hz, 2H, Ar-*H*), 7.26 (d, $^3J_{HH}$ = 8.0 Hz, 2H, Ar-*H*), 7.14 (d, $^3J_{HH}$ = 8.0 Hz, 1H, Ar-*H*), 6.67 (dd, $^3J_{HH}$ = 8.0 Hz, $^4J_{HH}$ = 4.0 Hz, 1H, Ar-*H*), 6.63 (d, $^4J_{HH}$ = 4.0 Hz, 1H, Ar-*H*), 4.74 (brs, 1H, C*H*OH), 3.76 (s, 3H, OCH_3), 3.35–3.27 (m, 2H, CH_2), 3.17–3.08 (m, 1H, CH_2), 2.73-2.49 (m, 7H, CH_2), 1.65 (brs, 4H, CH_2). ^{13}C{^{1}H}-NMR (CD_3OD): δ 160.26, 148.55, 141.78, 137.22, 130.23 (2C, *C*H),129.29 (q, $^2J_{CF}$ = 31.9 Hz, 1C, *C*CF), 127.67 (*C*H), 126.34 (q,$^3J_{CF}$ = 3.9 Hz, 2C, *C*HCHCF), 126.08 (q, $^1J_{CF}$ = 271.0 Hz, 1C, *C*F), 116.57 (*C*H), 111.72 (*C*H), 72.37 (OCH), 63.71 (*C*N), 60.11 (*C*N), 56.53 (*C*N), 55.75 (OCH$_3$), 36.58 (CH$_2$), 30.31 (CH$_2$), 27.24 (CH$_2$). HRMS calcd for $C_{22}H_{27}F_3NO_2$ [*M* + H]$^+$: *m*/*z* = 394.1994, found 394.1998; error: 1.0 ppm. HPLC (general method A): t_R = 7.21 min, purity 100%.

7-Methoxy-3-(4-(4-methoxyphenyl)butyl)-2,3,4,5-tetrahydro-1*H*-benzo[*d*]azepin-1-ol (L5). 7-Methoxy-2,3,4,5-tetrahydro-1*H*-benzo[*d*]azepin-1-ol (100 mg, 0.52 mmol), **T5** (270 mg, 0.81 mmol), and Na_2HPO_4 (430 mg, 3.0 mmol) were suspended in acetonitrile (2 mL) and heated at 90 °C for 2 d. Reaction progress was monitored with HPLC (general method A). The reaction mixture was then cooled to RT, passed through a 0.2 µm syringe filter, and purified with HPLC (general method C). The solvent was then removed under vacuum. The residue was then dissolved in acetonitrile, passed through a 0.2 µm syringe filter, and dried with Centrifan to give **L5** as white crystals (0.21 g, yield 87%). Mp: 86–89 °C. ^{1}H-NMR ($CDCl_3$): δ 7.18 (d, $^3J_{HH}$ = 8.0 Hz, 1H, Ar-*H*), 7.06 ($^3J_{HH}$ = 8 Hz, 2H, Ar-*H*), 6.81 ($^3J_{HH}$ = 8.0 Hz, 2H, Ar-*H*), 6.69 (dd, $^3J_{HH}$ = 8.0 Hz, $^4J_{HH}$ = 4.0 Hz, 1H, Ar-*H*), 6.62 (d, $^4J_{HH}$ = 4.0 Hz,

 doi:10.20944/preprints202604.0788.v2

1H, Ar-*H*), 4.83 (d, $^{3}J_{HH}$ = 4.0 Hz, 1H, C*H*OH), 3.77 (s, 3H, OCH_3), 3.76 (s, 3H, OCH_3), 3.37 (vt, $^{2}J_{HH}$ = 12 Hz, 1H, CH_2), 3.20–3.29 (m, 1H, CH_2), 3.15 (m, 1H, CH_2), 2.86–2.76 (m, 5H, CH_2), 2.57 (vt, $^{2}J_{HH}$ = 12 Hz, 2H, CH_2), 1.61 (m, 4H, CH_2). ^{13}C{^{1}H}-NMR (CDCl$_3$): δ 159.31, 158.02, 139.94, 134.24, 133.88, 129.56, 129.40 (2C, *C*H), 116.43 (*C*H), 114.00 (2C, *C*H), 111.01 (*C*H), 70.85 (*C*HO), 60.08 (*C*N), 59.39 (*C*N), 55.48 (*C*N), 55.41 (OCH$_3$), 34.65, 34.33, 29.09, 24.92, 21.20. HRMS calcd for $C_{22}H_{30}NO_3$ [*M* + H]$^+$: *m*/*z* = 356.2226, found 356.2223; error: –0.8 ppm. HPLC (general method A): t_R = 5.05 min, purity 99.52%.

7-Methoxy-3-(4-(4-methylphenyl)butyl)-2,3,4,5-tetrahydro-1*H*-benzo[*d*]azepin-1-ol (L6). Use of the method for **L5** with 7-methoxy-2,3,4,5-tetrahydro-1*H*-benzo[*d*]azepin-1-ol (130 mg, 0.67 mmol), **T6** (260 mg, 0.82 mmol), and Na_2HPO_4 (630 mg, 4.4 mmol) in acetonitrile (10 mL) gave **L6** as white crystals (88 mg, 37%). Mp: 86–87 °C. ^{1}H-NMR (CDCl$_3$): δ 7.11 (d, $^{3}J_{HH}$ = 12 Hz, 1H, Ar-*H*), 7.10 (AB, $^{3}J_{HH}$ = 8 Hz, 2H, Ar-*H*), 7.07 (AB, $^{3}J_{HH}$ = 8.0 Hz, 2H, Ar-*H*), 6.66 (dd, $^{3}J_{HH}$ = 8.0 Hz, $^{4}J_{HH}$ = 4.0 Hz, 1H, Ar-*H*), 6.54 (d, $^{4}J_{HH}$ = 4.0 Hz, 1H, Ar-*H*), 4.60 (d, $^{3}J_{HH}$ = 4.0 Hz, 1H, C*H*OH), 3.78 (s, 3H, OCH_3), 3.28 (vt, $^{2}J_{HH}$ = 12 Hz, 1H, CH_2), 3.20–3.16 (m, 1H, CH_2), 3.04–2.99 (m, 1H, CH_2), 2.69–2.58 (m, 5H, CH_2), 2.54 (d, $^{2}J_{HH}$ = 12 Hz, 1H, CH_2), 2.43 (vt, $^{2}J_{HH}$ = 12 Hz, 1H, CH_2), 2.32 (s, 3H, CH_3), 1.68–1.61 (m, 2H, CH_2), 1.59–1.53 (m, 2H, CH_2). ^{13}C{^{1}H}-NMR (CDCl$_3$): δ 159.14, 141.31, 139.36, 135.63, 135.41, 129.91, 129.23 (*C*H), 128.46 (*C*H), 116.79 (*C*H), 110.43 (*C*H), 72.49 (*C*HO), 60.92 (*C*N), 59.83 (*C*N), 56.24 (*C*N), 55.42 (OCH$_3$), 35.89, 35.48, 29.42, 26.70, 21.20 (CH$_3$). HRMS calcd for $C_{22}H_{30}NO_2$ [*M* + H]$^+$: *m*/*z* = 340.2277, found 340.2271; error: –1.8 ppm. HPLC (general method A): t_R = 6.27 min, purity 100%.

7-Methoxy-3-(4-(4-bromophenyl)butyl)-2,3,4,5-tetrahydro-1*H*-benzo[*d*]azepin-1-ol (L7). Use of the method for **L5** with 7-methoxy-2,3,4,5-tetrahydro-1*H*-benzo[*d*]azepin-1-ol (210 mg, 1.1 mmol), **T7** (400 mg, 1.04 mmol), and Na_2HPO_4 (700 mg, 4.9 mmol) in acetonitrile (2 mL) with heating at 90 °C for 5 d gave **L7** as a white crystals (0.35 g, yield 62%). Mp: 93–96 °C. ^{1}H-NMR (CDCl$_3$): δ 7.40 (d, $^{3}J_{HH}$ = 8.0 Hz, 2H, Ar-*H*), 7.11 (d, $^{3}J_{HH}$ = 8.0 Hz, 1H, Ar-*H*), 7.05 (d, $^{3}J_{HH}$ = 8.0 Hz, 2H, Ar-*H*), 6.66 (dd, $^{3}J_{HH}$ = 8.0 Hz, $^{4}J_{HH}$ = 4.0 Hz, 1H, Ar-*H*), 6.64 (d, $^{4}J_{HH}$ = 4.0 Hz, 1H, Ar-*H*), 4.62 (d, $^{3}J_{HH}$ = 4.0 Hz, 1H, C*H*OH), 3.77 (s, 3H, OCH$_3$), 3.28 (vt, $^{2}J_{HH}$ = 12 Hz, 1H, CH_2), 3.20–3.15 (m, 1H, CH_2), 3.04–2.99 (m, 1H, CH_2), 2.70–2.55 (m, 6H, CH_2), 2.46 (vt, $^{2}J_{HH}$ = 12 Hz, 1H, CH_2), 1.66–1.60 (m, 2H, CH_2), 1.58–1.53 (m, 2H, CH_2). ^{13}C{^{1}H}-NMR (CDCl$_3$): δ 159.16, 141.31, 141.13, 135.44, 131.59 (*C*H), 130.34 (*C*H), 129.87, 119.72 (*C*H), 116.76 (*C*H), 110.49 (*C*H), 72.36 (*C*HO), 60.85 (*C*N), 59.65 (*C*N), 56.19 (*C*N), 55.41 (OCH$_3$), 36.64, 35.29, 29.08, 26.48. HRMS calcd for $C_{21}H_{27}BrNO_2$ [*M* + H]$^+$: *m*/*z* = 404.1225, found 404.1229; error: 1.0 ppm. HPLC (general method A): t_R = 6.90 min, purity 96.64%.

7-Methoxy-3-(4-(4-fluorophenyl)butyl)-2,3,4,5-tetrahydro-1*H*-benzo[d]azepin-1-ol (L8). Use of the method for **L5** with 7-methoxy-2,3,4,5-tetrahydro-1*H*-benzo[*d*]azepin-1-ol (120 mg, 0.62 mmol), **T8** (260 mg, 0.81 mmol), and Na_2HPO_4 (450 mg, 3.2 mmol) in acetonitrile (2 mL) gave **L8** as a brown oil (0.23 g, yield 79%). ^{1}H-NMR (CDCl$_3$): δ 7.13 (d, $^{3}J_{HH}$ = 8.0 Hz, 2H, Ar-*H*), 7.11 (d, $^{3}J_{HH}$ = 8.0 Hz, 2H, Ar-*H*), 6.96 (t, $^{3}J_{HH}$ = $^{3}J_{HF}$ = 8.0 Hz, 2H, Ar-*H*), 6.65 (d, $^{3}J_{HH}$ = 8.0 Hz, 1H, Ar-*H*), 6.63 (brs, 1H, Ar-*H*), 4.62 (d, $^{3}J_{HH}$ = 4.0 Hz, 1H, C*H*OH), 3.77 (s, 3H, OCH_3), 3.27 (vt, $^{2}J_{HH}$ = 12 Hz, 1H, CH_2), 3.19–3.15 (m, 1H, CH_2), 3.03–2.99 (m, 1H, CH_2), 2.70–2.55 (m, 6H, CH_2), 2.46 (vt, $^{2}J_{HH}$ = 12 Hz, 1H, CH_2), 1.67–1.60 (m, 2H, CH_2), 1.58–1.53 (m, 2H, CH_2). ^{13}C{^{1}H}-NMR (CDCl$_3$): δ 162.64 (*C*-F), 160.23 (*C*-F), 159.16, 141.13, 137.97, 137.94, 135.46, 129.89 (*C*H, J_{CF}), 129.81 (*C*H, J_{CF}), 116.75 (*C*H), 115.36 (*C*H, J_{CF}), 115.15 (*C*H, J_{CF}), 110.49 (*C*H), 72.34 (*C*HO), 60.86 (*C*N), 59.69 (*C*N), 56.17 (*C*N), 55.41 (OCH$_3$), 36.65, 35.07, 29.37, 26.47. HRMS calcd for $C_{21}H_{27}NO_2F$ [*M* + H]$^+$: *m*/*z* = 344.2026, found 344.2025; error: –0.3 ppm. HPLC (general method A): t_R = 5.55 min, purity 98.74%.

7-Methoxy-3-(4-(naphthalen-2-yl)butyl)-2,3,4,5-tetrahydro-1*H*-benzo[*d*]azepin-1-ol (L9). Use of the method for **L7** with7-methoxy-2,3,4,5-tetrahydro-1*H*-benzo[*d*]azepin-1-ol (100 mg, 0.52 mmol), **X9** (250 mg, 0.71 mmol), and Na_2HPO_4 (280 mg, 2.0 mmol) in acetonitrile (10 mL) gave **L9** as white crystals (0.14 g, yield 74%). Mp: 86–88 °C. ^{1}H-NMR (CDCl$_3$): δ 7.81 (d, $^{3}J_{HH}$ = 8.0 Hz, 1H, Nap-*H*), 7.78 (d, $^{3}J_{HH}$ = 8.0 Hz, 1H, Nap-*H*), 7.77 (d, $^{3}J_{HH}$ = 8.0 Hz, 1H, Nap-*H*), 7.60 (s, 1H, Nap-*H*), 7.44 (p, $^{3}J_{HH}$ = 7.0 Hz, 2H, Nap-*H*), 7.31 (d, $^{3}J_{HH}$ = 8.0 Hz, 1H, Ar-*H*), 7.14 (d, $^{3}J_{HH}$ = 8.0 Hz, 1H, Ar-*H*), 6.68 (dd, $^{3}J_{HH}$ = 8.0 Hz, $^{4}J_{HH}$ = 4.0 Hz, 1H, Ar-*H*), 6.63 (d, $^{4}J_{HH}$ = 4.0 Hz, 1H, Ar-*H*), 4.72 (d, $^{3}J_{HH}$ = 4.0 Hz, 1H, C*H*OH), 3.76 (s, 3H, OCH_3), 3.34 (vt, $^{2}J_{HH}$ = 12 Hz, 1H, CH_2), 3.29–3.24 (m, 1H, CH_2), 3.11–3.07 (m, 1H, CH_2), 2.81–2.66 (m, 6H, CH_2), 2.57 (vt, $^{2}J_{HH}$ = 12 Hz, 1H, CH_2), 1.78–1.70 (m, 2H, CH_2), 1.69–1.62 (m, 2H, CH_2).

 doi:10.20944/preprints202604.0788.v2

$^{13}C\{^{1}H\}$-NMR ($CDCl_3$): δ 159.20, 139.69, 134.96, 133.78, 132.19, 129.79 (*C*H), 129.09, 128.12 (*C*H), 127.79 (*C*H), 127.61 (*C*H), 127.40 (*C*H), 126.68 (*C*H), 126.11 (*C*H), 125.34 (*C*H), 116.61 (*C*H), 110.67 (*C*H), 71.66 (*C*HO), 60.57 (*C*N), 59.62 (*C*N), 55.91 (*C*N), 55.40 (OCH_3), 35.89, 35.69, 28.91, 25.89. HRMS calcd for $C_{25}H_{30}NO_2$ [*M* + H]$^+$: *m*/*z* = 376.2277, found 376.2272; error: –1.3 ppm. HPLC (general method A): t_R = 5.69 min, purity 99.13%.

3-(4-(Pyridin-2-yl)butyl)-7-methoxy-2,3,4,5-tetrahydro-1*H*-benzo[*d*]azepin-1-ol (L10). *Method 1*. 7-Methoxy-2,3,4,5-tetrahydro-1*H*-benzo[*d*]azepin-1-ol (15.3 mg, 0.52 mmol), **T10** (39.7 mg, 0.66 mmol), and Na_2HPO_4 (73.3 mg, 2.0 mmol) were suspended in DMSO (1.0 mL). The reaction mixture was then heated in a microwave reactor (three conditions were utilized: i) 80 °C 10 min, 30 W, 250 psi; ii) 120 °C, 10 min, 50 W, 250 psi; iii) 150 °C, 10 min, 60 W, 250 psi). Only a by-product was formed. LC-MS (Scheme 8) indicated this to be a cyclized product from the attack of the pyridinyl nitrogen on the tosylate leaving group of **T10**.

Method 2. 7-Methoxy-2,3,4,5-tetrahydro-1*H*-benzo[*d*]azepin-1-ol (150 mg, 0.52 mmol), **T10** (300 mg, 0.66 mmol) and Na_2HPO_4 (510 mg, 2.0 mmol) were suspended in acetonitrile (10 mL) and heated at 90 °C for 22 d. Only by-product was formed. Again, LC-MS indicated that this was produced by-intramolecular cyclization of **X10** (Scheme 8).

7-Methoxy-3-(4-(pyridin-2-yl)but-3-yn-1-yl)-2,3,4,5-tetrahydro-1*H*-benzo[*d*]azepin-1-ol (L11). Use of the method for **L7** in the same molar proportions with **T11** (240 mg, 0.80 mmol) gave **L11** a brown oil (0.268 g, yield 77%). ^{1}H-NMR (CD_3OD): δ 8.34 (ddd, $^{3}J_{HH}$ = 5.0 Hz, 1 H, Ar-*H*), 7.68 (td, $^{3}J_{HH}$ = 7.8 Hz, $^{4}J_{HH}$ = 1.8 Hz, 1H, Ar-*H*), 7.37 (vt, $^{3}J_{HH}$ = 7.9 Hz, 1H, Ar-*H*), 7.23 (dd, $^{3}J_{HH}$ = 7.7 Hz ,1 H, Ar-*H*), 7.17 (d, $^{3}J_{HH}$ = 8.4 Hz, 1H, Ar-*H*), 6.62 (dd, $^{3}J_{HH}$ = 8.3 Hz, $^{4}J_{HH}$ = 2.7 Hz, 1H, Ar-*H*), 6.57 (d, $^{4}J_{HH}$ = 2.6 Hz, 1H, Ar-*H*), 4.67 (d, $^{3}J_{HH}$ = 7.6 Hz, 1H, C*H*OH), 3.66 (s, 3H, OCH_3), 2.92 (m, 1H, CH_2), 2.83 (m, 3H, CH_2), 2.73 (m, 3H, CH_2), 2.59 (m, 3H, CH_2). $^{13}C\{^{1}H\}$-NMR in (CD_3OD): δ 160.35, 150.42 (*C*H), 144.54, 142.03, 138.66, 137.06, 128.66 (*C*H), 128.37 (*C*H), 124.42 (*C*H), 116.76 (*C*H), 111.69 (*C*H), 91.08 81. 69, 72.97 (*C*HO), 63.09 (*C*N), 58.77 (*C*N), 56.21 (*C*N), 55.76 (OCH_3), 36.99 (CH_2), 18.12 (CH_2). HRMS calcd for $C_{20}H_{23}N_2O_2$ [*M* + H]$^+$: *m*/*z* = 323.1760, found 323.1757; error: –0.9 ppm. HPLC (general method B): t_R = 6.50 min, purity 100%.

3-(4-(6-Fluoropyridin-2-yl)but-3-yn-1-yl)-7-methoxy-2,3,4,5-tetrahydro-1*H*-benzo[*d*]azepin-1-ol (L12). 7-Methoxy-2,3,4,5-tetrahydro-1*H*-benzo[*d*]azepin-1-ol (134 mg, 0.69 mmol) and **X12** (274 mg, 0.86 mmol) were mixed and then heated in a microwave reactor (135 °C,10 min, 60 W, 250 psi) to give a black solid upon cooling to RT. The solid was dissolved in DMF (3 mL), passed through a 0.2 μm syringe, and then purified with HPLC (general method C). The solvent was then removed under vacuum. The residue was redissolved in acetonitrile, passed through a 0.2 μm syringe filter, and then dried with Centrifan to give **L12** as a brown oil (29 mg, yield 12%). ^{1}H-NMR ($CDCl_3$) δ 7.70 (dd, $^{3}J_{HH}$ = 8.0 Hz, $^{3}J_{HF}$ = 16.0, 1H, Ar-*H*), 7.28 (dd, $^{3}J_{HH}$ = 7.1 Hz, $^{4}J_{HH}$ = 1.8 Hz, 1H, Ar-*H*), 7.11 (d, $^{3}J_{HH}$ = 7.9 Hz, 1H, Ar-*H*), 6.86 (dd, $^{3}J_{HH}$ = 8.3 Hz, $^{4}J_{HH}$ = 2.5 Hz, 1H, Ar-*H*), 6.67 (dd, $^{3}J_{HH}$ = 8.3 Hz, $^{4}J_{HH}$ = 2.6 Hz, 1H, Ar-*H*), 6.65 (s, 1H, Ar-*H*), 4.63 (d, $^{3}J_{HH}$ = 6.8 Hz, 1H, C*H*-OH), 3.78 (s, 3H, OCH_3), 3.27 (m, 2H, CH_2), 3.09 (m, 1H, CH_2), 2.96 (t, $^{3}J_{HH}$ = 7.1 Hz, 2H, CH_2), 2.68 (m, 4H, CH_2), 2.58 (t, $^{3}J_{HH}$ = 12.0 Hz, 1H, CH_2). $^{13}C\{^{1}H\}$-NMR($CDCl_3$): δ 163.08 (d, $^{1}J_{CF}$ = 240 Hz, 1C, *C*F), 159.18, 141.62 (d, $^{3}J_{CF}$ = 15.1 Hz, 1C, *C*NCF), 141.37 (d, $^{3}J_{CF}$ = 8.2 Hz, 1C, *C*HCHCF), 141.19, 135.50, 130.06, 124.54 (d, $^{4}J_{CF}$ = 4.2 Hz, 1C, *C*HCHCHCF), 116.87 (*C*H), 110.50 (*C*H), 109.22 (d, $^{2}J_{CF}$ = 36.7 Hz, 1C, *C*HCF), 90.15, 80.64, 72.73 (*C*HO), 60.70 (*C*N), 58.07 (*C*N), 55.96 (*C*N), 55.42 (OCH_3), 37.32 (CH_2), 18.27 (CH_2). HRMS calcd for $C_{20}H_{22}N_2O_2F$ [*M* + H]$^+$: *m*/*z* = 341.1665, found 323.1667. error: 0.6 ppm. HPLC (general method B): t_R = 7.60 min, purity 98.69%.

3-(2-(Benzofuran-2-yl)ethyl)-7-methoxy-2,3,4,5-tetrahydro-1*H*-benzo[*d*]azepin-1-ol (L13). 7-Methoxy-2,3,4,5-tetrahydro-1*H*-benzo[*d*]azepin-1-ol (100 mg, 0.52 mmol), **T13** (184 mg, 0.582 mmol) and Na_2HPO_4 (250 mg, 1.76 mmol) were suspended in acetonitrile (10 mL) and heated at 90 °C for 22 d to give **L13** as a brown oil (139 mg, yield 71%). ^{1}H-NMR (CD_3OD): δ 7.48 (dd, $^{3}J_{HH}$ = 7.1 Hz, $^{4}J_{HH}$ = 1.4, 1H, Ar-*H*), 7.39 (d, $^{3}J_{HH}$ = 8.1 Hz, 1H, Ar-*H*), 7.28 (d, $^{3}J_{HH}$ = 8.3 Hz, 1H, Ar-*H*), 7.20 (td, $^{3}J_{HH}$ = 7.3 Hz, $^{4}J_{HH}$ = 1.4 Hz, 1H, Ar-*H*), 7.16 (td, $^{3}J_{HH}$ = 7.4 Hz, $^{4}J_{HH}$ = 1.2 Hz, 1H, Ar-*H*), 6.73 (dd, $^{3}J_{HH}$ = 8.3 Hz, $^{4}J_{HH}$ = 2.6 Hz, 1H, Ar-*H*), 6.68 (d, $^{4}J_{HH}$ = 2.6 Hz, 1H, Ar-*H*), 6.53 (s, 1H, Ar-*H*), 4.79 (d, $^{3}J_{HH}$ = 8.0 Hz, 1H, C*H*OH), 3.77 (s, 3H, OCH_3), 3.03 (t, $^{3}J_{HH}$ = 3.1 Hz, 4H, CH_2), 2.97 (m, 2H, CH_2), 2.86 (m, 2H, CH_2), 2.78

 doi:10.20944/preprints202604.0788.v2

(t, $^3J_{HH}$ = 11.7 Hz, 1H, CH_2), 2.66 (t, $^3J_{HH}$ = 10.5 Hz, 1H, CH_2). ^{13}C{^{1}H}-NMR (CD_3OD): δ 160.31, 158.78, 156.28, 141.96, 137.06, 130.40, 128.27 (*C*H), 124.54 (*C*H), 123.72 (*C*H), 121.51 (*C*H), 116.75 (*C*H), 111.67 (*C*H), 103.90 (*C*H), 72.82 (*C*HO), 63.21 (*C*N), 58.41 (*C*N), 56.28 (*C*N) 55.75 (OCH_3), 36.87 (CH_2), 27.00 (CH_2). HRMS calcd for $C_{21}H_{24}NO_3$ [*M* + H]$^+$: *m*/*z* = 338.1756, found 338.1751. error: –1.5 ppm. HPLC (general method A): t_R = 4.59 min, purity 97.52%

3-(2-(5-Bromobenzofuran-2-yl)ethyl)-7-methoxy-2,3,4,5-tetrahydro-1*H*-benzo[*d*]azepin-1-ol (L14). Use of the method for **L12** in the same molar proportions with **T14** (142 mg, 0.359 mmol) gave **L14** as a brown oil (76 mg, yield 51%). ^{1}H-NMR ($CDCl_3$): δ 7.61 (s, 1H, Ar-*H*), 7.33 (AB, $^3J_{HH}$ = 8.0 Hz, 1H, Ar-*H*), 7.27 (AB, $^3J_{HH}$ = 8.0 Hz, 1H, Ar-*H*), 7.21 (d, $^3J_{HH}$ = 8.0 Hz, 1H, Ar-*H*), 7.13 (d, $^3J_{HH}$ = 8.0 Hz, 1H, Ar-*H*), 6.72 (d, $^3J_{HH}$ = 8.0 Hz, 1H, Ar-*H*), 6.65 (s, 1H, Ar-*H*), 6.46 (s, 1H, Ar-*H*), 4.92 (brs, 1H, C*H*OH), 3.78 (s, 3H, OCH_3), 3.34 (brs, 2H, CH_2), 3.21 (brs, 2H, CH_2), 3.13 (q, $^3J_{HH}$ = 8.0 Hz, 2H, CH_2), 2.75–2.69 (m, 2H, CH_2), 1.32 (t, $^3J_{HH}$ = 8.0 Hz, 2H, CH_2). ^{13}C{^{1}H}-NMR ($CDCl_3$): δ 159.30, 153.68, 130.84 (*C*H), 130.07, 129.12, 126.67 (CH), 126.13, 123.35 (*C*H), 116.77 (*C*H), 115.95 (*C*H), 112.46 (*C*H), 110.73 (*C*H), 103.10 (*C*Br), 72.03 (*C*HO), 60.52 (*C*N), 57.72 (*C*N), 56.00 (*C*N), 55.45 (OCH_3), 45.90, 26.33. HRMS calcd for $C_{21}H_{23}BrNO_3$ [*M* + H]$^+$: *m*/*z* = 416.0861, found 416.0865; error: 1.0 ppm. HPLC (general method A): t_R = 6.52 min, purity 100%.

3-(2-(5-Fluorobenzofuran-2-yl)ethyl)-7-methoxy-2,3,4,5-tetrahydro-1*H*-benzo[*d*]azepin-1-ol (L15). Use of the method for **L12** in the same molar proportions with **T15** (214 mg, 0.640 mmol) gave **L16** as a brown wax (134 mg, yield 59%). ^{1}H-NMR (CD_3OD): δ 7.38 (dd, $^3J_{HH}$ = 3.9 Hz, 1H, Ar-*H*), 7.26 (d, $^3J_{HH}$ = 8.3 Hz, 1H, Ar-*H*), 7.20 (dd, $^3J_{HH}$ = 8.8, $^4J_{HH}$ = 2.4 Hz, 1H, Ar-*H*), 6.96 (td, $^3J_{HH}$ = 9.3 Hz, $^4J_{HH}$ = 2.9 Hz, 1H, Ar-*H*), 6.74 (dd, $^3J_{HH}$ = 8.4 Hz, $^4J_{HH}$ = 2.4 Hz, 1H, Ar-*H*), 6.71 (d, $^4J_{HH}$ = 2.4 Hz, 1H, Ar-*H*), 6.58 (s, 1H, Ar-*H*), 4.82 (t, $^3J_{HH}$ = 4.6 Hz C*H*-OH), 3.77 (s, 3H, O-CH_3), 3.13 (br, 5H, CH_2), 2.95 (br, 5H, CH_2). ^{13}C{^{1}H}-NMR (CD_3OD): δ 160.78 (d, $^1J_{CF}$ = 235 Hz, 1C, *C*F), 160.66, 159.93, 152.60, 141.64, 136.24, 131.29 (d, $^3J_{CF}$ = 11.0 H, 1C, *C*HCHCF), 129.17, 116.94 (*C*H), 112.53 (d, $^3J_{CF}$ = 9.9 Hz, 1C, *C*HCHCF), 112.20 (*C*H), 111.95 (*C*H), 107.06 (d, $^2J_{CF}$ = 25.2 Hz, 1C, *C*HCF), 104.71 (d, $^4J_{CF}$ = 3.7 Hz, 1C, *C*HCHCHCF), 72.34 (*C*HO), 62.21 (*C*N), 58.09 (*C*N), 56.62 (*C*N), 55.80 (OCH_3), 35.75 (CH_2), 26.43 (CH_2). HRMS calcd for $C_{21}H_{23}NO_3F$ [*M* + H]$^+$: *m*/*z* = 356.1662, found 356.1658; error: –1.1 ppm. HPLC (general method A): t_R = 5.38 min, purity 99.57%.

3-(2-(5-Trifluoromethylbenzofuran-2-yl)ethyl)-7-methoxy-2,3,4,5-tetrahydro-1*H*-benzo[*d*]azepin-1-ol (L16). Use of the method for **L11** in the same molar proportions with **T16** (178 mg, 0.463 mmol) gave **L16** as a thick brown oil (120 mg, yield 64%). ^{1}H-NMR (CD_3OD): δ 7.85 (s, 1H, Ar-*H*), 7.58 (AB, $^3J_{HH}$ = 8.6 Hz, 1H, Ar-*H*), 7.52 (AB, $^3J_{HH}$ = 8.6 Hz, $^4J_{HH}$ = 1.5 Hz, 1H, Ar-*H*), 7.28 (d, $^3J_{HH}$ = 8.4 Hz, 1H, Ar-*H*), 6.73 (dd, $^3J_{HH}$ = 8.4 Hz, $^4J_{HH}$ = 2.6 Hz, 1H, Ar-*H*), 6.68 (m, $^3J_{HH}$ = 4.0 Hz, 2H, Ar-*H*), 4.78 (d, $^3J_{HH}$ = 7.6 Hz, 1H, C*H*-OH), 3.77 (s, 3H, OCH_3), 3.06 (m, 4H, CH_2), 2.99 (m, 1H, CH_2), 2.95 (m, 1H, CH_2), 2.83 (m, 2H, CH_2), 2.77 (m, 1H, CH_2), 2.67 (m, 1H, CH_2). ^{13}C{^{1}H}-NMR (CD_3OD): δ 161.42, 160.34, 157.71 (d, $^4J_{CF}$ = 1.67 Hz, 1C, *C*HCHCHCF), 141.96, 130.75, 128.28 (*C*H), 126.41 (q, $^1J_{CF}$ = 270.0 Hz, 1C, *C*F), 126.41 (q, $^2J_{CF}$ = 31.4 Hz, 1C, *C*HCF), 121.64 (q, $^3J_{CF}$ = 3.6 Hz, 1C, *C*HCHCF), 119.15 (q, $^3J_{CF}$ = 4.3 Hz, 1C, *C*HCHCF), 116.74 (*C*H), 112.35 (*C*H), 111.68 (*C*H), 104.31 (*C*H), 72.89 (*C*HO), 63.23 (*C*N), 58.14 (*C*N), 56.28 (*C*N), 55.75 (OCH_3), 36.87 (CH_2), 27.03 (CH_2). HRMS calcd for $C_{22}H_{23}NO_3F_3$ [*M* + H]$^+$: *m*/*z* = 406.1630, found 406.1625; error: –1.2 ppm. HPLC (general method A): t_R = 6.81 min, purity 96.43%

3-(4-(Benzofuran-2-yl)butyl)-7-methoxy-2,3,4,5-tetrahydro-1*H*-benzo[*d*]azepin-1-ol (L17). Use of the method for **L12** in same molar proportions with **T17** (257 mg, 0.746 mmol) gave **L17** as white crystals (194 mg, yield 71%). Mp: 90–92 °C. ^{1}H-NMR (CD_3OD): δ 7.47 (dd, $^3J_{HH}$ = 7.0 Hz, $^4J_{HH}$ = 1.9 Hz, 1H, Ar-*H*), 7.37 (d, $^3J_{HH}$ = 8.0 Hz, 1H, Ar-*H*), 7.29 (d, $^3J_{HH}$ = 8.5 Hz, 1H, Ar-*H*), 7.18 (td, $^3J_{HH}$ = 7.2 Hz, $^4J_{HH}$ = 1.5 Hz, 1H, Ar-*H*), 7.14 (td, $^3J_{HH}$ = 7.3 Hz, $^4J_{HH}$ = 1.3 Hz, 1H, Ar-*H*), 6.72 (dd, $^3J_{HH}$ = 8.4 Hz, $^4J_{HH}$ = 2.6 Hz, 1H, Ar-*H*), 6.66 (d, $^4J_{HH}$ = 2.6 Hz, 1H, Ar-*H*), 6.47 (d, $^4J_{HH}$ = 0.6 Hz, 1H, Ar-*H*), 4.79 (d, $^3J_{HH}$ = 8.1 Hz, 1H, C*H*-OH), 3.75 (s, 3H, OCH_3), 2.89 (m, 6H, CH_2), 2.60 (m, 3H, CH_2), 2.44 (br, 1H, CH_2), 1.79 (quint, 2H, CH_2), 1.65 (quint, 2H, CH_2). ^{13}C{^{1}H}-NMR (CD_3OD): δ 160.59, 160.24, 156.28, 141.79, 137.22, 130.50 (*C*H), 127.68 (*C*H), 124.38, 123.64, 121.41 (*C*H), 116.57 (*C*H), 111.71 (*C*H), 111.62 (*C*H), 103.26 (*C*H), 72.37 (*C*HO), 63.70 (*C*N), 60.01 (*C*N), 56.52 (*C*N), 55.75 (OCH_3), 36.51 (CH_2), 29.18 (CH_2), 27.20

 doi:10.20944/preprints202604.0788.v2

(CH_2), 26.89 (CH_2). HRMS: calcd for $C_{23}H_{28}NO_3$ [M + H]$^+$: m/z = 366.2069, found 366.2069; error: 0.0 ppm. HPLC (general method A): t_R = 6.34 min, purity 99.00%.

7-Methoxy-3-(4-(5-(trifluoromethyl)benzofuran-2-yl)butyl)-2,3,4,5-tetrahydro-1*H*-benzo[*d*]azepin-1-ol (L18). Use of the method for **L12** in same molar proportions with **T18** (197 mg, 0.478 mmol) gave **L18** as a thick brown oil (141 mg, yield 68%). ^{1}H-NMR (CD_3OD): δ 7.83 (s, 1H, Ar-*H*), 7.56 (AB, $^3J_{HH}$ = 8.6 Hz, 1H, Ar-*H*), 7.51 (AB, $^3J_{HH}$ = 8.6 Hz, $^4J_{HH}$ = 1.3 Hz, 1 H, Ar-*H*), 7.29 (d, $^3J_{HH}$ = 8.4 Hz, 1 H, Ar-*H*), 6.72 (dd, $^3J_{HH}$ = 8.4 Hz, $^4J_{HH}$ = 2.6 Hz, 1 H, Ar-*H*), 6.67 (d, $^4J_{HH}$ = 2.5 Hz, 1 H, Ar-*H*), 6.63 (d, $^4J_{HH}$ = 0.8 Hz, 1 H, Ar-*H*), 4.79 (d, $^3J_{HH}$ = 7.8 Hz, 1H, C*H*-OH), 3.76 (s, 3H, OCH_3), 2.90 (m, 6H, CH_2), 2.61 (br, 3H, CH_2), 2.51 (br, 1H, CH_2), 1.82 (quint, $^3J_{HH}$ = 7.8 Hz, 2H, CH_2), 1.67 (quint, $^3J_{HH}$ = 7.8 Hz, 2H, CH_2). ^{13}C{^{1}H}-NMR (CD_3OD): δ 163.13, 160.28, 157.71, 144.77, 137.15, 130.83, 127.78 (CH), 126.44 (q, $^1J_{CF}$ = 270.8 Hz, 1C, *C*F), 126.35 (q, $^2J_{CF}$ = 31.6 Hz, 1C, *C*HCF), 121.52 (q, $^3J_{CF}$ = 3.7 Hz, 1C, *C*HCHCF), 119.06 (q, $^3J_{CF}$ = 4.1 Hz, 1C, *C*HCHCF), 116.59 (CH), 112.30 (CH), 111.73 (CH), 103.64 (CH), 72.39 (CHO), 63.60 (CN), 59.94 (CN), 56.56 (CN), 55.75 (OCH$_3$), 36.46 (CH_2), 29.14 (CH_2), 27.15 (CH_2), 26.70 (CH_2). HRMS calcd for $C_{23}H_{28}NO_3$ [M + H]$^+$: m/z = 434.1943, found 434.1948; error: 1.2 ppm. HPLC (general method A): t_R = 8.06 min, purity 98.37%.

Methyl 3-((4-(4-(1-hydroxy-7-methoxy-1,2,4,5-tetrahydro-3*H*-benzo[*d*]azepin-3-yl)butyl)phenyl)thio)propanoate (L19). L2 (0.2067 g, 0.458 mmol), methyl 3-mercaptopropanoate (62 µL, d = 1.085 g/mL, 0.560 mmol), *N*,*N*,1,1,1-pentamethylstannanamine (90 µL, 0.552 mmol), and $Pd(PPh_3)_4$ (120 mg, 0.104 mmol) were dissolved in DMSO (4.0 mL). and then heated in a microwave reactor (110 °C, 10 min, 50 W, 250 psi). LC-MS analysis showed consumption of the starting material **L2,** and this was confirmed with HPLC (general method A). The reaction mixture was purified with HPLC (general method D). The product fractions were collected, dried under vacuum, redissolved in ethanol, passed through a 0.2 µm syringe filter, and then dried with Centrifan to give **L19** as a brown wax (174.3 mg, yield 86%). ^{1}H-NMR (CD_3OD): δ 7.30 (d, $^3J_{HH}$ = 6.7 Hz, 2H, Ar-*H*), 7.30 (t, $^3J_{HH}$ = 4.5 Hz, 1H, Ar-*H*), 7.16 (d, $^3J_{HH}$ = 8.2 Hz, 2H, Ar-*H*), 6.73 (dd, $^3J_{HH}$ = 8.3 Hz, $^4J_{HH}$ = 2.6 Hz, 1H, Ar-*H*), 6.67 (d, $^4J_{HH}$ = 2.5 Hz, 1H. Ar-*H*), 4.79 (d, $^3J_{HH}$ = 8.0 Hz, 1H, C*H*OH), 3.76 (s, 3H, OCH_3), 3.65 (s, 3H, OCH_3), 3.11 (t, $^3J_{HH}$ = 7.1 Hz, 2H, CH_2), 2.88 (m, 4H, CH_2), 2.61 (m, 8H, CH_2), 1.63 (m, 4H, CH_2). ^{13}C{^{1}H}-NMR (CD_3OD): δ 174.10 (*C*=O), 160.31, 142.71, 141.71, 138.65, 137.04, 133.59 (CH), 132.03 (CH), 130.43 (CH), 127.88 (CH), 116.61 (CH), 111.76 (CH), 72.24 (OCH), 63.45 (CN), 60.18 (CN), 56.55 (CN), 55.77 (OCH$_3$), 52.36 (OCH$_3$), 36.29 (CH_2), 35.34 (CH_2), 30.92 (CH_2), 30.62 (CH_2), 30.44 (CH_2), 27.04 (CH_2). HRMS calcd for $C_{25}H_{34}NO_4S$ [M + H]$^+$: m/z = 444.2209, found 444.2203. error: –1.4 ppm. HPLC (general method A): t_R = 6.46 min, purity 97.56%.

7-Methoxy-3-(4-(4-(4,4,5,5-tetramethyl-1,3,2-dioxaborolan-2-yl)phenyl)butyl)-2,3,4,5-tetrahydro-1*H*-benzo[*d*]azepin-1-ol (L20). *Method 1.* Iodo compound **L2** (105.7 mg, 0.234 mmol), 4,4,4',4',5,5,5',5'-octamethyl-2,2'-bi(1,3,2-dioxaborolane) (86.9 mg, 0.342 mmol), KOAc (83.7 mg, 0.853 mmol), and DPPF-$PdCl_2$·CH_2Cl_2 (34.8 mg, 0.0426 mmol) were dissolved in DMSO (3.0 mL) and heated in a microwave reactor (80 °C, 60 min, 60 W, 250 psi). LC-MS analysis showed consumption of the starting material **L2** and this was confirmed with HPLC (general method A). The reaction mixture was purified with HPLC (general method D). A saturated NaCl solution was immediately added to each product fraction as they eluted, followed by a saturated $NaHCO_3$ solution to prevent decomposition. The aqueous phase was then extracted with acetonitrile and dried ($MgSO_4$), filtered, and then dried under vacuum. The residue was redissolved in ethanol, passed through a 0.2 µm syringe filter, and then dried with Centrifan to give **L20** as a purple wax (39.0 mg, yield 37%). ^{1}H-NMR (CD_3CN): δ 7.63 (d, $^3J_{HH}$ = 7.7 Hz, 2H, Ar-*H*), 7.23 (d, $^3J_{HH}$ = 7.6 Hz, 2H, Ar-*H*), 7.17 (d, $^3J_{HH}$ = 8.0 Hz, 1H, Ar-*H*), 6.68 (m, 2H, Ar-*H*), 4.61 (d, $^3J_{HH}$ = 7.3 Hz, 1H, C*H*OH), 3.74 (s, 3H, OCH_3), 2.85 (m, 1H, CH_2), 2.73 (m, 2H, CH_2), 2.65 (m, 2H, CH_2), 2.58 (m, 2H, CH_2), 1.64 (q, $^3J_{HH}$ = 7.6 Hz, 2H, CH_2), 1.54 (m, 2H, CH_2), 1.31 (s, 12H, CH_3). ^{13}C{^{1}H}-NMR (CD_3CN): δ 159.27, 146.85, 136.67, 135.12, 128.70 (CH), 128.57 (CH), 117.88 (CH), 116.35 (CH), 110.76 (CH), 84.23 (*C*OC$_3$), 72.02 (*C*OH), 62.06 (CN), 59.21 (CN), 55.98 (CN), 55.35 (OCH$_3$), 36.29 (CH_2), 35.94 (CH_2), 29.27 (CH_2), 26.68 (CH_2), 24.77 (CH_3). HRMS calcd for $C_{27}H_{39}BNO_4$ [M+H]$^+$: m/z = 452.2972, found 452.2976; error: 0.9 ppm. HPLC (general method A): t_R = 7.64 min, purity 76.67%.

 doi:10.20944/preprints202604.0788.v2

Method 2. Bromo compound **L7** (18.7 mg, 0.0462 mmol), 4,4,4',4',5,5,5',5'-octamethyl-2,2'-bi(1,3,2-dioxaborolane) (57 mg, 0.224 mmol), KOAc (7.9 mg, 0.0805 mmol), and DPPF-$PdCl_2$·CH_2Cl_2 (13.2 mg, 0.0162 mmol) were dissolved in DMSO (0.5 mL).and then heated in a microwave reactor (110 °C, 30 min, 50 W, 250 psi). LC-MS analysis showed consumption of the starting material **L7**and this was confirmed with HPLC (general method A). The reaction mixture was purified with HPLC (general method D), and the collected fractions were dried under vacuum. The product was redissolved in ethanol, passed through a 0.2 μm syringe filter, and then dried with Centrifan to give **L20** as a purple wax (11.2 mg, yield 54%).

Infrared/Vibrational Circular Dichroism. The enantiomers of **L3** were subjected to a computational infrared (IR) and vibrational circular dichroism (VCD) study to allow comparison of computed spectra with those determined experimentally, and to define the absolute configurations of the enantiomers (see Supplementary Information). Chiral HPLC (general method E) showed two enantiomers: enantiomer 1 (t_R = 8.05 min, 48.03%); enantiomer 2 (t_R = 13.22 min, 48.06%). The enantiomers were purified with chiral HPLC (general method F). Enantiomer 1: chiral HPLC (general method E) (t_R = 8.10 min, 98.01%), $[\alpha]D^{20}$ = –39.02° (*c* 1.0, $CHCl_3$), $[\alpha]D^{20}$ = +8.89° (*c* 1.0, EtOH). Enantiomer 2: chiral HPLC (general method E): t_R = 13.27 min, 99.19%), $[\alpha]D^{20}$ = +34.03° (*c* 1.0, $CHCl_3$), $[\alpha]D^{20}$ = –3.67° (*c* 1.0, EtOH). The first eluting enantiomer in chiral HPLC analysis (general method E) was found to be the *S*-enantiomer.

Verification of the absolute configuration of enantiomers of L6, L2, L19, and L20 by stereo-retentive transformations originating from (*S*)-L3.

Synthesis of (*S*)-L19 from (*S*)-L2. Chiral HPLC analysis (general method E) of racemic **L2** showed (*S*)**-L2** (t_R = 6.97 min, 50.35%) and (*R*)**-L2** (t_R = 10.96 min, 47.92%). The enantiomers were separated with preparative chiral HPLC (general method F). Analytical chiral HPLC (general method E) for (*S*)**-L2** showed t_R = 6.89 min. (HPLC purity 98.14%); $[\alpha]D^{20}$ = –24.45° (*c* 1.0, $CHCl_3$).Chiral HPLC (general method E) for (*R*)-**L2** showed t_R = 11.24 min (HPLC purity 99.2%); $[\alpha]D^{20}$ = +28.57° (*c* 1.0, $CHCl_3$),

For the synthesis of (*S*)-**L19**, compound (*S*)-**L2** (46.8 mg, 103.7 μmol), methyl 3-((trimethylstannyl)thio)propanoate (26.7 μL, 124.4 μmol), triethylamine (14.5 μL, 103.7 μmol), and [1,1′-bis(diphenylphosphino)ferrocene]dichloropalladium(II) (35.5 mg, 48.52 μmol) were dissolved in acetonitrile (1 mL). The reaction mixture was then heated in a microwave reactor (90 °C. 20 min, 120 W, 250 psi) and purified with HPLC (method G) to give compound (*S*)-**L19** as a brown oil (38.8 mg, 84.4%). Analytical chiral HPLC (general method E) showed t_R = 14.04 min (purity 97.24%), This synthesis was repeated on (*R*)-**L2** to give (*R*)-**L19**.

Analytical chiral HPLC (general method E): (*S*)-**L19**, t_R = 13.91 min, 50.24%; (*R*)-**L19**, t_R = 21.48 min, 48.23%, $[\alpha]D^{20}$ = +2.47° (*c* 1.0, $CHCl_3$). Analysis of synthesized (*R*)-**L19** showed t_R = 20.25 min (97.71%), $[\alpha]D^{20}$ = –1.81° (*c* 1.0, $CHCl_3$).

Synthesis of (*S*)-L3 from (*S*)-L19. Analytical chiral HPLC (general method E) of racemic **L3** showed two compounds: enantiomer 1 (t_R = 8.05 min, 48.03%) and enantiomer 2 (t_R = 13.22 min, 48.06%). (*S*)-**L3** was prepared from (*S*)-**L19** to assign an absolute configuration to each enantiomer**,** as follows.

Compound (*S*)**-L19** (27.4 mg, 61.77 μmol) in DCM (1 mL) was mixed with methyl iodide (3.86 μL, 61.77 μmol) and 1 M tetra-*n*-butylammonium hydroxide (TBAOH; 129.7 μL, 129.7 μmol) and stirred at RT for 20 min. The reaction mixture was then diluted with DCM (5 mL) and washed thrice with water (10 mL). The solvent was removed by rotary evaporation. The residue was dissolved in DCM (1 mL) and purified with HPLC (general method F) to give compound (*S*)-**L3** as white crystals (17.3 mg, 75.4%); m.pt. 88–90 °C; analytical chiral HPLC (general method E): t_R = 8.10 min, purity 98.01%. $[\alpha]D^{20}$ = –39.02° (*c* 1.0, $CHCl_3$), $[\alpha]D^{20}$ = +8.89° (*c* 1.0, EtOH). The synthesis was repeated with (*R*)-**L19** to give (*R*)-**L3**. Analytical *c*hiral HPLC (general method E): t_R = 13.27 min, 99.19%. $[\alpha]D^{20}$ = +34.03° (*c* 1.0, $CHCl_3$), $[\alpha]D^{20}$ = –3.67° (*c* 1.0, EtOH).

The enantiomers of racemic **L3** were separated with chiral HPLC (general method F). Co-injections of racemic **L3** with each synthesized **L3** enantiomer confirmed their retention times.

 doi:10.20944/preprints202604.0788.v2

Synthesis of (*S*)-L20 from (*S*)-L2. Compound (*S*)-**L2** (138 mg, 306 μmol), bis(pinacolato)diborane (200 mg, 788 μmol), potassium acetate (51.2 mg, 521 μmol), and [1,1′-bis(diphenylphosphino)ferrocene]dichloropalladium(II) (62.8 mg, 85.8 μmol) were dissolved in acetonitrile (3 mL). The reaction mixture was then heated in a microwave reactor (80 °C, 20 min, 150 W, 250 psi). and passed through a 0.2 μm syringe filter and purified with normal phase HPLC in three equal portions (method G). Fractions containing the product were immediately neutralized with saturated aqueous sodium bicarbonate (1 mL), extracted with ethyl acetate, and dried to give (*S*)-**L20** (43 mg, 31%) as a purple wax. Analytical chiral HPLC (general method E): t_R = 6.0 min, purity 93.5% (see Supporting Information). (*R*)-**L20** was likewise synthesized from (*R*)-**L2** Analytical chiral HPLC (general method E): t_R = 8.81 min, purity 92.0% (see Supporting Information).

Synthesis of (*S*)-L6 from (*S*)-L20. Analytical chiral HPLC of **L6** (general method E) showed enantiomer 1 (t_R = 5.76 min, 44.43%) and enantiomer 2 (t_R = 9.44 min, 51.46%). The assignment of absolute configuration of each **L6** enantiomer was achieved by preparing (*S*)-**L6** from (*S*)-**L20**, as follows.

Compound (*S*)-**L20** (20.0mg, 44.3 μmol) was dissolved in methanol (0.4 mL). Cesium fluoride (199.4 μmol) in methanol (1 M; 199.4 μL), methyl iodide (3.04 μL, 48.8 μmol), and tetrakis(triphenylphosphine)palladium(0) (5.2 mg, 4.50 μmol) were dissolved in acetonitrile (0.6 mL). The reaction mixture was then heated in a microwave reactor (90 °C, 20 min, 80 W, 250 psi), then passed through a 0.2 μm syringe filter, and purified by HPLC (method G) to give (*S*)-**L6** as a brown oil (12.6 mg, 83.9%); $[\alpha]D^{20}$ = –24.23° (*c* 1.0, $CHCl_3$). Analytical chiral HPLC (general method E): t_R = 5.93 min, purity 98.28%.

(*R*)-**L6** was likewise synthesized from (*R*)-**L20**; $[\alpha]D^{20}$ = +28.23° (*c* 1.0, $CHCl_3$). Chiral HPLC analysis (general method E): t_R = 9.57 min (99.28%).

Methylation of L19 to synthesize L3 under conditions mimicking a ^{11}C-labeling reaction. A stock solution of **L19** in DMF (1.25 mg/mL) was prepared and 0.4 mL of this solution was transferred to a V-vial. A stock solution of iodomethane in DMF (1% v/v; 1 mL) was prepared and 7.0 μL of this solution was added to the **L19** solution and stirred for 2 min. TBAOH in methanol (1 M; 5.0 μL) was then added and this was stirred at RT for 5 min. LC-MS showed complete conversion of **L19** into **L3**. The solution was then dried with Centrifan, and the reaction mixture dissolved in ethanol (0.1 mL) for chiral HPLC (general method E) and LC-MS analysis.

Methylation of L20 to L6 under conditions mimicking a ^{11}C-labeling reaction. $Pd_2(dba)_3$ and P(*o*,*p*-tol)$_3$ were mixed in the weight ratio of 1: 1.33. A portion of this mixture (0.6 mg; 0.562 μmol Pd) was taken and placed in a vial. A solution of **L20** in methanol (1.25 mg/mL; 0.40 mL) was added, followed by a solution of iodomethane in methanol (10% w/w; 7 μL). A stock solution (20 μL) of cesium fluoride in methanol (1 M) was then added to the reaction mixture, which was heated at 80 °C for 90 min. LC-MS showed consumption of the starting material (**L20**) and product formation (**L6**). The reaction mixture was then purified with reversed phase HPLC (general method C) and the product dried with Centrifan. The purified product was analyzed with chiral HPLC (general method E) and LC-MS.

In Vitro Binding Assays

PDSP binding assays. Selected compounds from early in the project were assayed by the National Institutes of Health (NIH) Psychoactive Drug Screening Program (PDSP) for K_i at rat brain GluN2B subtype (https://pdspdb.unc.edu/pdspweb/). The assay was performed either manually or automatically.

A suspension of transient transfected mouse fibroblast cell membrane homogenates was prepared as reported at a concentration of ~500,000 cells/mL. This suspension was sonicated, and aliquots (100 μL) were added to each of four tubes (total 48 in a rack). A solution of [^{3}H]ifenprodil (2.22 TBq/mmol, 0.01 kBq/μL; ARC, https://arcincusa.com/) in PBS (100 μL) was added to each tube. Ifenprodil or other displacer (test compound) was dissolved in DMSO to give a 1-mM stock solution, which was further diluted with DMSO to give solutions ranging in known concentration from 10^{-5} to

 doi:10.20944/preprints202604.0788.v2

10^{-10} M. Then 10 µL of each solution was added to a separate tube. The content of each tube was then diluted to 1.0 mL with PBS, vortexed, and incubated at 37 °C for 2 h. After separation of tube contents with a cell harvester, filter paper (GF/B; Whatman; Derwood, MD), pretreated with 0.5% polyethyleneimine solution, was washed with PBS (3 mL × 3). Each filter was then placed in a 7-mL plastic vial. Scintillation fluid (4 mL) was added to each vial. The scintillation vials were incubated overnight and then counted for radioactivity. The data were analyzed with Prism 7 version 7.03 (GraphPad Software; San Diego, CA) with 'One site competition' curve-fitting. K_i values were calculated according to the Cheng-Prusoff equation [37]: $K_i = IC_{50}/(1 + [L]/K_D)$ where [L] is the concentration (0.4 nM) and K_D the equilibrium dissociation constant (7.6 nM) of the reference radioligand. The latter was determined with 'Scatchard analysis' of homologous displacement from multiple runs with self-displacement from membrane homogenates.

In-house binding assay. The assay procedure with [^{3}H]ifenprodil as reference radioligand was the same as above but with a different protein source. The rat brain was homogenized in PBS (1×) at 1: 24, and the protein concentration measured. The protein concentration used for the binding assay ranged from 0.8 to 3.5 mg/mL. A solution of [^{3}H]ifenprodil (2.22 TBq/mmol, 0.01 kBq/µL) in PBS (100 µL) was added to each tube (10 nM).

Supplementary Materials: The following supporting information can be downloaded at the website of this paper posted on Preprints.org, NMR spectra; HPLC general methods; analytical and preparative HPLC chromatograms, including chiral HPLC chromatograms; ligand physicochemical properties used in CNS PET MPO scoring; docking of ifenprodil.

Author Contributions: LC, SC, LM, and AW, chemistry and analysis; LC, pharmacology; LC, study concept; YL, computational chemistry; LC and VWP, project supervision and manuscript drafting; all authors contributed to analysis of data and manuscript writing and reviewed the final manuscript.

Acknowledgments: We thank John Lloyd (NIDDK Advanced Mass Spectrometry Facility) for high-resolution mass spectrometry measurements, Peter Herscovitch (NIH Clinical PET Center) for radioisotope production. K_i determinations were generously provided by the National Institute of Mental Health's Psychoactive Drug Screening Program, Contract # HHSN-271-2013-00017-C (NIMH PDSP). The NIMH PDSP is Directed by Bryan L. Roth, PhD at the University of North Carolina at Chapel Hill and Project Officer Jamie Driscoll at NIMH, Bethesda, MD, USA.

Funding: This study was supported by the Intramural Research Programs of the National Institutes Health (NIH) (project: ZIAMH002793 to VWP). The contributions of the NIH authors were made as part of their official duties as NIH federal employees and comply with agency policy requirements. They are considered Works of the United States Government. However, the findings and conclusions presented in this paper are those of the authors and do not necessarily reflect the views of the NIH or the U.S. Department of Health and Human Services.

Declaration of Generative A1 and A1-Asssited Technology in Manuscript Preparation: During the preparation of this work the authors used ChatGPT to improve language and presentation. After use of this tool the authors reviewed and edited the contents as needed and take full responsibility for the contents of the published article.

Abbreviations

DCM, dichloromethane; DMF, *N*,*N*′-dimethylformamide; DMSO, dimethyl sulfoxide; MW, microwave; NIMH, National Institute of Mental Health; NMDA, *N*-methyl-D-aspartate; PDSP, psychoactive drug screening program; RT, room temperature; THF; tetrahydrofuran; TFA, trifluoroacetic acid; VCD/IR, vibrational circular dichroism/infrared; USP, Unites States Pharmacopeia.

 doi:10.20944/preprints202604.0788.v2

References

1. Hansen, K.B.; Yi, F.; Perszyk, R.E.; Furukawa H. Structure, function, and allosteric modulation of NMDA receptors. *J. Gen. Physiol.* **2018**, *87*, 1081-1105. DOI: 10.1085/jgp.201812032
2. Li, X.H.; Miao, H.H.; Zhuo, M. NMDA Receptor Dependent Long-term Potentiation in Chronic Pain. *Neurochem. Res.* **2018**, *3*, 531-538. DOI: 10.1007/s11064-018-2614-8
3. Ueda, K.; Serajee, F.; Huq, A.M. Clinical Benefit of NMDA Receptor Antagonists in a Patient With ATP1A2 Gene Mutation. *Pediatrics* **2018**, *141*, S390-S394. DOI: 10.1542/peds.2017-0852
4. Zhou, Q.; Sheng, M. NMDA receptors in nervous system diseases. *Neuropharmacology* **2013**, *74*, 69-75. DOI: 10.1016/j.neuropharm.2013.03.030
5. Song, X.; Jensen, M.O.; Jogini, V.; Stein, R.A.; Lee, C.-H.; Mchaourab, H.S.; Shaw, D.E.; Gouaux, E. Mechanism of NMDA receptor channel block by MK-801 and memantine. *Nature* **2018**, *556*, 515-519. DOI: 10.1038/s41586-018-0039-9
6. Folch, J.; Busquets, O.; Ettcheto, M.; Sánchez-López, E.; Castro-Torres, R.D.; Verdaguer, E.; Garcia, M.L.; Olloquequi, J.; Casadesús, G.; Beas-Zarate, C.; Pelegri, C.; Vilaplana, J.; Auladell, C.; Camins, A. Memantine for the Treatment of Dementia: A Review on its Current and Future Applications. *J. Alzheimers Dis.* **2018**, *62*, 1223-1240. DOI: 10.3233/JAD-170672
7. Zhuo, M. Ionotropic glutamate receptors contribute to pain transmission and chronic pain. *Neuropharmacology* **2017**, *112*, 228-234. DOI: 10.1016/j.neuropharm.2016.08.014
8. Chazot, P.L. The NMDA receptor NR2B subunit: a valid therapeutic target for multiple CNS pathologies. *Curr. Med. Chem.* **2004**, *11*, 389-396. DOI: 10.2174/0929867043456061
9. Monaco, S,A.; Gulchina, Y.; Gao, W.J.. NR2B subunit in the prefrontal cortex: A double-edged sword for working memory function and psychiatric disorders. *Neurosci. Biobehav. Rev.* **2015**, *56*, 127-138. DOI: 10.1016/j.neubiorev.2015.06.022
10. Politis, M.; Piccini, P. Positron emission tomography imaging in neurological disorders. *J. Neurol.* **2012**, *259*, 1769-1780. DOI: 10.1007/s00415-012-6428-3
11. Hooker, J.M.; Carson, R.E. Human Positron Emission Tomography Neuroimaging. *Annu. Rev. Biomed. Eng.* **2019**, *21*, 551-581. DOI: 10.1146/annurev-bioeng-062117-121056
12. Pike, V.W. Overview of clinically available radiotracers for imaging in neurodegenerative disorders. In: Cross, D.J; .Mosci, K.; Minoshima, S.; eds. *Molecular Imaging of Neurodegenerative Disorders*. Switzerland AG Springer; **2023**, Chapter 3, 35-55. DOI: 10.1007/978-3-031-35098-6 (book DOI)
13. Ferrando, R.; Hernandes, D.; Ghini, B.G.; Coutinho, A.M. PET Imaging in Psychiatric Disorders. *Semin. Nucl. Med.* **2025**, *55*, 587-604. DOI: 10.1053/j.semnuclmed.2025.06.004
14. Naganawa, M.; Gallezot, J.D.; Rossano, S.; Carson, R.E. Quantitative PET Imaging in Drug Development: Estimation of Target Occupancy. *Bull. Math. Biol.* **2019**, *81*, 3508-3541. DOI: 10.1007/s11538-017-0374-2
15. Ghosh, K.K.; Padmanabhan, P.; Yang, C.T.; Ng, D.C.E.; Palanivel, M.; Mishra, S.; Halldin, C.; Gulyás, B. Positron emission tomographic imaging in drug discovery. *Drug Discov. Today* **2022**, *27*, 280-291. DOI: 10.1016/j.drudis.2021.07.025
16. Pike, V.W. PET radiotracers: crossing the blood-brain barrier and surviving metabolism. *Trends Pharmacol. Sci.* **2009**, *30*, 431-440. DOI: 10.1016/j.tips.2009.05.005
17. Zhang, L.; Villalobos, A.; Beck, E.M.; Bocan, T.; Chappie, T.A.; Chen, L.; Grimwood, S.; Heck, S.D.; Helal, C.J.;.Hou, X.; Humphrey, J.M.; Lu, J.; Skaddam, M.B.; McCarthy, T.J.; Verhoest, P.R.; Wager, T.T.; Zasadny, K.. Design and Selection Parameters to Accelerate the Discovery of Novel Central Nervous System Positron Emission Tomography (PET) Ligands and Their Application in the Development of a Novel Phosphodiesterase 2A PET Ligand. *J. Med. Chem.* **2013**, *56*, 4568-4579. DOI: 10.1021/jm400312y
18. Pike, V,W. Considerations in the Development of Reversibly Binding PET Radioligands for Brain Imaging. *Curr. Med, Chem.* **2016**, *23*, 1818-1869. DOI: 10.2174/0929867323666160418114826
19. Kassenbrock, A.; Vasdev, N.; Liang, S.H. Selected PET Radioligands for Ion Channel Linked Neuroreceptor Imaging: Focus on GABA, NMDA and nACh Receptors. *Curr. Top. Med. Chem.* **2016**, *16*, 1830-1842. DOI: 10.2174/1568026616666160315142457
20. Fu, H.; Chen, Z.; Josephson, L.; Li, Z.; Liang, S.H. Positron Emission Tomography (PET) Ligand Development for Ionotropic Glutamate Receptors: Challenges and Opportunities for Radiotracer Targeting

 doi:10.20944/preprints202604.0788.v2

N-methyl-D-aspartate (NMDA), a-Amino-3-hydroxy-5-methyl-4-isoxazolepropionic Acid (AMPA) and Kainate Receptors. *J. Med. Chem.* **2018**; *62*, 403-419. DOI: 10.1021/acs.jmedchem.8b00714

21. Erlandsson, K.; Galovic, M. Recent Progress in NMDA Glutamate Receptor Imaging. In: Sone, D. ed. *Molecular Imaging for Brain Diseases*. Vol 222. New York: Humana; **2025**, 1-20. DOI: 10.1007/978-1-0716-4494-2 (book DOI)
22. Kim, J.H.; Marton, J.; Ametamey, S.M.; Cumming, P. A. Review of Molecular Imaging of Glutamate Receptors. *Molecules* **2020**, *25*, 4749. DOI: 10.3390/molecules25204749
23. Rischka, L.; Vraka. C.; Pichler, V.; Rasul, S.; Nics, L; Gryglewski, G.; Handschuh, P.; Murgaš, M.; Godbersen, G.M.; Silberbauer, L.R., Unterholzner, J.; Wotawa, C.; Haider, A; Ahmed, H.; Schibli, R; Mindt, T.; Mitterhauser, M.; Wadsak, W.; Hahn, A.; Lanzenberger, R.; Hacker, M.; Ametamey, S.M. First-in-Humans Brain PET Imaging of the GluN2B-Containing *N*-methyl-D-aspartate Receptor with (*R*)-^{11}C-Me-NB1. .*J. Nucl. Med.* **2022**, *63*, 936-941. DOI: 10.2967/jnumed.121.262427
24. Cai, L; Liow, J.S.; Morse, C.L.; Telu, S.; Davies, R.; Frankland, M.P.; Zoghbi, S.S.; Cheng, K.; Hall, M.D.; Innis, R.B.; Pike,V.W. Evaluation of ^{11}C-NR2B-SMe and its Enantiomers as PET Radioligands for Imaging the NR2B Subunit within the NMDA Receptor Complex in Rats. *J. Nucl. Med.* **2020**, *61*, 1212-1220. DOI: 10.2967/jnumed.119.235143
25. Cai, L.; Liow, J.S.; Morse, C.L.; Telu, S.; Davies, R ; Manly, L.S.; Zoghbi, S.S.; Chin. F.T.; Innis, R.B.; Pike, V.W. Candidate 3-benzazepine-1-ol type GluN2B receptor radioligands (^{11}C-NR2B-Me enantiomers) have high binding in cerebellum but not to sigma1 receptors. *EJNMMI Res.* **2023**; *13*, 28. DOI: 10.1186/s13550-023-00975-6
26. Smart, K.; Zheng, M.Q.; Ahmed, H.; Fang, H.; Xu, Y.; Cai, L; Holden, D.; Kapinos, M.; Haider, A.; Felchner, Z.; Ropchan, J.R.; Tamagnan, G.; Innis, R.B.; Pike, V.W.; Ametamey, S.M.; Huang, Y.; Carson, R.E. Comparison of three novel radiotracers for GluN2B-containing NMDA receptors in non-human primates: (*R*)-[^{11}C]NR2B-Me, (*R*)-[^{18}F]of-Me-NB1, and (*S*)-[^{18}F]of-NB1. *J. Cereb. Blood Flow Metab.* **2022**, *42*, 1398-1409. DOI: 10.1177/0271678X221084416
27. Karakas, E.; Furukawa, H. Crystal structure of a heterotetrameric NMDA receptor ion channel. *Science* **2014**, *344*, 992-997. DOI: 10.1126/science.1251915
28. Karakas, E.; Simorowski, N.; Furukawa. H. Subunit arrangement and phenylethanolamine binding in GluN1/GluN2B NMDA receptors. *Nature* **2011**, *475*, 249-253. DOI: 10.1038/nature10180
29. Burger, P.B.; Yuan; H.; Karakas, E.; Geballe, M.; Furukawa, H.; Liotta, D.C.; Snyder J.P.; Traynelis, S.F. Mapping the binding of GluN2B-selective *N*-methyl-D-aspartate receptor negative allosteric modulators. *Mol. Pharmacol.* **2012**, *82*, 344-359. DOI: 10.1124/mol.112.078568
30. Korff, M.; Steigerwald,.R; Bechthold E, Schepmann, D.; Schreiber, J.A.; Meuth, S.G.; Seebohm, G.; Wünsch, B. Chemical, pharmacodynamic and pharmacokinetic characterization of the GluN2B receptor antagonist 3-(4-phenylbutyl)-2,3,4,5-tetrahydro-1*H*-3-benzazepine-1,7-diol - starting point for PET tracer development. *Biol Chem.* 2023;404:279-289. DOI: 10.1515/hsz-2022-0222
31. Tewes, B.; Frehland, B.; Schepmann. D.; Schmidtke, K.U.; Winckler, T.; Wunsch, B. Conformationally constrained NR2B selective NMDA receptor antagonists derived from ifenprodil: Synthesis and biological evaluation of tetrahydro-3-benzazepine-1,7-diols. *Bioorg. Med. Chem.* **2010**, *18*, 8005-8015. DOI: 10.1016/j.bmc.2010.09.026
32. Tewes, B.; Frehland, B.; Schepmann, D.; Robaa, D.; Uengwetwanit, T.; Gaube, F., Winckler, T.; Sippl W.; Wünsch, B. Enantiomerically Pure 2-Methyltetrahydro-3-benzazepin-1-ols Selectively Blocking GluN2B Subunit Containing *N*-Methyl-D-aspartate Receptors. *J. Med. Chem.* **2015**, *58*, 6293-6305. DOI: 10.1021/acs.jmedchem.5b00897
33. Borgel, F.;Szermerski, M.; Schreiber, J.A.; Temme, L.; Strutz-Seebohm, N.; Lehmkuhl, K.; Schepmann, D.; Ametamey, S.M.; Seebohm, G.; Schmidt, T. J.; Wünsch, B. Synthesis and Pharmacological Evaluation of Enantiomerically Pure GluN2B Selective NMDA Receptor Antagonists. *ChemMedChem.* **2018**, *13*, 1580-1587. DOI: 10.1002/cmdc.201800214
34. Kramer, S.D.; Betzel, T.; Mu, L.; Haider, A.; Müller Herde, A.; Boninsegni, A.K.; Keller, C.; Szermerski, M.; Schibli, R.; Wünsch, B.; Ametamey, S.M. Evaluation of ^{11}C-Me-NB1 as a Potential PET Radioligand for

 doi:10.20944/preprints202604.0788.v2

Measuring GluN2B-Containing NMDA Receptors, Drug Occupancy, and Receptor Cross Talk. *J. Nucl. Med.* **2018**, *59*, 698-703. DOI: 10.2967/jnumed.117.200451

35. Alluri, S.R.; Zheng, M.-Q.; Holden, D.; Ahmed, H.; Felchner, Z.; Kapinos, M.; Carson, R.E., Ametamey, S.M. ; Huang, Y. Characterization of [^{18}F]PF-NB1 Enantiomers for Imaging NMDA GluN2B Receptors in Nonhuman Primates and Comparison with Analogous ^{18}F-labeled Radiotracers. *ACS Chem. Neurosci.* **2026**, *17*, 251–259. DOI: 10.1021/acschemneuro.5c00840
36. Bechthold, E.; Schreiber, J.A.; Lehmkuhl, K.; Frehland, B.; Schepmann, D.; Bernal, F.A.; Daniliuc, C.; Álvarez, I.; Val Garcia, C.; Schmidt, T.J.; Seebohm, G.; Wünsch, B. Ifenprodil Stereoisomers: Synthesis, Absolute Configuration, and Correlation with Biological Activity. *J. Med. Chem.* **2021**, *64*, 1170-1179. DOI: 10.1021/acs.jmedchem.0c01912
37. Cheng, Y.; Prusoff, W.H. Relationship between Inhibition Constant (K_I) and Concentration of Inhibitor Which Causes 50 Per Cent Inhibition (I_{50}) of an Enzymatic-Reaction. *Biochem. Pharmacol.* **1973**, *22*, 3099-3108. . DOI: 10.1016/0006-2952(73)90196-2